

Observation of Three Resonant Structures in the Cross Section of $e^+e^- \rightarrow \pi^+\pi^- h_c$

- M. Ablikim¹, M. N. Achasov^{4,c}, P. Adlarson⁷⁷, X. C. Ai⁸², R. Aliberti³⁶, A. Amoroso^{76A,76C}, Q. An^{73,59,a}, Y. Bai⁵⁸, O. Bakina³⁷, Y. Ban^{47,h}, H.-R. Bao⁶⁵, V. Batozskaya^{1,45}, K. Begzsuren³³, N. Berger³⁶, M. Berlowski⁴⁵, M. Bertani^{29A}, D. Bettom^{30A}, F. Bianchi^{76A,76C}, E. Bianco^{76A,76C}, A. Bortone^{76A,76C}, I. Boyko³⁷, R. A. Briere⁵, A. Brueggemann⁷⁰, H. Cai⁷⁸, M. H. Cai^{39,k,l}, X. Cai^{1,59}, A. Calcaterra^{29A}, G. F. Cao^{1,65}, N. Cao^{1,65}, S. A. Cetin^{63A}, X. Y. Chai^{47,h}, J. F. Chang^{1,59}, G. R. Che⁴⁴, Y. Z. Che^{1,59,65}, C. H. Chen⁹, Chao Chen⁵⁶, G. Chen¹, H. S. Chen^{1,65}, H. Y. Chen²¹, M. L. Chen^{1,59,65}, S. J. Chen⁴³, S. L. Chen⁴⁶, S. M. Chen⁶², T. Chen^{1,65}, X. R. Chen^{32,65}, X. T. Chen^{1,65}, X. Y. Chen^{12,g}, Y. B. Chen^{1,59}, Y. Q. Chen¹⁶, Y. Q. Chen³⁵, Z. J. Chen^{26,i}, Z. K. Chen⁶⁰, S. K. Choi¹⁰, X. Chu^{12,g}, G. Cibinetto^{30A}, F. Cossio^{76C}, J. Cottee-Meldrum⁶⁴, J. J. Cui⁵¹, H. L. Dai^{1,59}, J. P. Dai⁸⁰, A. Dbeysi¹⁹, R. E. de Boer³, D. Dedovich³⁷, C. Q. Deng⁷⁴, Z. Y. Deng¹, A. Denig³⁶, I. Denysenko³⁷, M. Destefanis^{76A,76C}, F. De Mori^{76A,76C}, B. Ding^{68,1}, X. X. Ding^{47,h}, Y. Ding³⁵, Y. Ding⁴¹, Y. X. Ding³¹, J. Dong^{1,59}, L. Y. Dong^{1,65}, M. Y. Dong^{1,59,65}, X. Dong⁷⁸, M. C. Du¹, S. X. Du⁸², S. X. Du^{12,g}, Y. Y. Duan⁵⁶, P. Egorov^{37,b}, G. F. Fan⁴³, J. J. Fan²⁰, Y. H. Fan⁴⁶, J. Fang⁶⁰, J. Fang^{1,59}, S. S. Fang^{1,65}, W. X. Fang¹, Y. Q. Fang^{1,59}, R. Farinelli^{30A}, L. Fava^{76B,76C}, F. Feldbauer³, G. Felici^{29A}, C. Q. Feng^{73,59}, J. H. Feng¹⁶, L. Feng^{39,k,l}, Q. X. Feng^{39,k,l}, Y. T. Feng^{73,59}, M. Fritsch³, C. D. Fu¹, J. L. Fu⁶⁵, Y. W. Fu^{1,65}, H. Gao⁶⁵, X. B. Gao⁴², Y. Gao^{73,59}, Y. N. Gao^{47,h}, Y. N. Gao²⁰, Y. Y. Gao³¹, S. Garbolino^{76C}, I. Garzia^{30A,30B}, P. T. Ge²⁰, Z. W. Ge⁴³, C. Geng⁶⁰, E. M. Gersabeck⁶⁹, A. Gilman⁷¹, K. Goetzen¹³, J. D. Gong³⁵, L. Gong⁴¹, W. X. Gong^{1,59}, W. Gradl³⁶, S. Gramigna^{30A,30B}, M. Greco^{76A,76C}, M. H. Gu^{1,59}, Y. T. Gu¹⁵, C. Y. Guan^{1,65}, A. Q. Guo³², L. B. Guo⁴², M. J. Guo⁵¹, R. P. Guo⁵⁰, Y. P. Guo^{12,g}, A. Guskov^{37,b}, J. Gutierrez²⁸, K. L. Han⁶⁵, T. T. Han¹, F. Hanisch³, K. D. Hao^{73,59}, X. Q. Hao²⁰, F. A. Harris⁶⁷, K. K. He⁵⁶, K. L. He^{1,65}, F. H. Heinsius³, C. H. Heinz³⁶, Y. K. Heng^{1,59,65}, C. Herold⁶¹, P. C. Hong³⁵, G. Y. Hou^{1,65}, X. T. Hou^{1,65}, Y. R. Hou⁶⁵, Z. L. Hou¹, H. M. Hu^{1,65}, J. F. Hu^{57,j}, Q. P. Hu^{73,59}, S. L. Hu^{12,g}, T. Hu^{1,59,65}, Y. Hu¹, Z. M. Hu⁶⁰, G. S. Huang^{73,59}, K. X. Huang⁶⁰, L. Q. Huang^{32,65}, P. Huang⁴³, X. T. Huang⁵¹, Y. P. Huang¹, Y. S. Huang⁶⁰, T. Hussain⁷⁵, N. Hüskens³⁶, N. in der Wiesche⁷⁰, J. Jackson²⁸, Q. Ji¹, Q. P. Ji²⁰, W. Ji^{1,65}, X. B. Ji^{1,65}, X. L. Ji^{1,59}, Y. Y. Ji⁵¹, Z. K. Jia^{73,59}, D. Jiang^{1,65}, H. B. Jiang⁷⁸, P. C. Jiang^{47,h}, S. J. Jiang⁹, T. J. Jiang¹⁷, X. S. Jiang^{1,59,65}, Y. Jiang⁶⁵, J. B. Jiao⁵¹, J. K. Jiao³⁵, Z. Jiao²⁴, S. Jin⁴³, Y. Jin⁶⁸, M. Q. Jing^{1,65}, X. M. Jing⁶⁵, T. Johansson⁷⁷, S. Kabana³⁴, N. Kalantar-Nayestanaki⁶⁶, X. L. Kang⁹, X. S. Kang⁴¹, M. Kavatsyuk⁶⁶, B. C. Ke⁸², V. Khachatryan²⁸, A. Khoukaz⁷⁰, R. Kiuchi¹, O. B. Kolcu^{63A}, B. Kopf³, M. Kuessner³, X. Kui^{1,65}, N. Kumar²⁷, A. Kupsc^{45,77}, W. Kühn³⁸, Q. Lan⁷⁴, W. N. Lan²⁰, T. T. Lei^{73,59}, M. Lellmann³⁶, T. Lenz³⁶, C. Li⁴⁴, C. Li⁴⁸, C. Li^{73,59}, C. H. Li⁴⁰, C. K. Li²¹, D. M. Li⁸², F. Li^{1,59}, G. Li¹, H. B. Li^{1,65}, H. J. Li²⁰, H. N. Li^{57,j}, Hui Li⁴⁴, J. R. Li⁶², J. S. Li⁶⁰, K. Li¹, K. L. Li²⁰, K. L. Li^{39,k,l}, L. J. Li^{1,65}, Lei Li⁴⁹, M. H. Li⁴⁴, M. R. Li^{1,65}, P. L. Li⁶⁵, P. R. Li^{39,k,l}, Q. M. Li^{1,65}, Q. X. Li⁵¹, R. Li^{18,32}, S. X. Li¹², T. Li⁵¹, T. Y. Li⁴⁴, W. D. Li^{1,65}, W. G. Li^{1,a}, X. Li^{1,65}, X. H. Li^{73,59}, X. L. Li⁵¹, X. Y. Li^{1,8}, X. Z. Li⁶⁰, Y. Li²⁰, Y. G. Li^{47,h}, Y. P. Li³⁵, Z. J. Li⁶⁰, Z. Y. Li⁸⁰, H. Liang^{73,59}, Y. F. Liang⁵⁵, Y. T. Liang^{32,65}, G. R. Liao¹⁴, L. B. Liao⁶⁰, M. H. Liao⁶⁰, Y. P. Liao^{1,65}, J. Libby²⁷, A. Limphirat⁶¹, C. C. Lin⁵⁶, D. X. Lin^{32,65}, L. Q. Lin⁴⁰, T. Lin¹, B. J. Liu¹, B. X. Liu⁷⁸, C. Liu³⁵, C. X. Liu¹, F. Liu¹, F. H. Liu⁵⁴, Feng Liu⁶, G. M. Liu^{57,j}, H. Liu^{39,k,l}, H. B. Liu¹⁵, H. H. Liu¹, H. M. Liu^{1,65}, Huihui Liu²², J. B. Liu^{73,59}, J. J. Liu²¹, K. Liu⁷⁴, K. Liu^{39,k,l}, K. Y. Liu⁴¹, Ke Liu²³, L. C. Liu⁴⁴, Lu Liu⁴⁴, M. H. Liu^{12,g}, P. L. Liu¹, Q. Liu⁶⁵, S. B. Liu^{73,59}, T. Liu^{12,g}, W. K. Liu⁴⁴, W. M. Liu^{73,59}, W. T. Liu⁴⁰, X. Liu⁴⁰, X. Liu^{39,k,l}, X. K. Liu^{39,k,l}, X. Y. Liu⁷⁸, Y. Liu⁸², Y. Liu⁸², Y. Liu^{39,k,l}, Y. B. Liu⁴⁴, Z. A. Liu^{1,59,65}, Z. D. Liu⁹, Z. Q. Liu⁵¹, X. C. Lou^{1,59,65}, F. X. Lu⁶⁰, H. J. Lu²⁴, J. G. Lu^{1,59}, X. L. Lu¹⁶, Y. Lu⁷, Y. H. Lu^{1,65}, Y. P. Lu^{1,59}, Z. H. Lu^{1,65}, C. L. Luo⁴², J. R. Luo⁶⁰, J. S. Luo^{1,65}, M. X. Luo⁸¹, T. Luo^{12,g}, X. L. Luo^{1,59}, Z. Y. Lv²³, X. R. Lyu^{65,p}, Y. F. Lyu⁴⁴, Y. H. Lyu⁸², F. C. Ma⁴¹, H. L. Ma¹, J. L. Ma^{1,65}, L. L. Ma⁵¹, L. R. Ma⁶⁸, Q. M. Ma¹, R. Q. Ma^{1,65}, R. Y. Ma²⁰, T. Ma^{73,59}, X. T. Ma^{1,65}, X. Y. Ma^{1,59}, Y. M. Ma³², F. E. Maas¹⁹, I. MacKay⁷¹, M. Maggiora^{76A,76C}, S. Malde⁷¹, Q. A. Malik⁷⁵, H. X. Mao^{39,k,l}, Y. J. Mao^{47,h}, Z. P. Mao¹, S. Marcello^{76A,76C}, A. Marshall⁶⁴, F. M. Melendi^{30A,30B}, Y. H. Meng⁶⁵, Z. X. Meng⁶⁸, G. Mezzadri^{30A}, H. Miao^{1,65}, T. J. Min⁴³, R. E. Mitchell²⁸, X. H. Mo^{1,59,65}, B. Moses²⁸, N. Yu. Muchnoi^{4,c}, J. Muskalla³⁶, Y. Nefedov³⁷, F. Nerling^{19,e}, L. S. Nie²¹, I. B. Nikolaev^{4,c}, Z. Ning^{1,59}, S. Nisar^{11,m}, Q. L. Niu^{39,k,l}, W. D. Niu^{12,g}, C. Normand⁶⁴, S. L. Olsen^{10,65}, Q. Ouyang^{1,59,65}, S. Pacetti^{29B,29C}, X. Pan⁵⁶, Y. Pan⁵⁸, A. Pathak¹⁰, Y. P. Pei^{73,59}, M. Pelizaeus³, H. P. Peng^{73,59}, X. J. Peng^{39,k,l}, Y. Y. Peng^{39,k,l}, K. Peters^{13,e}, K. Petridis⁶⁴, J. L. Ping⁴², R. G. Ping^{1,65}, S. Plura³⁶, V. Prasad³⁴, V. Prasad³⁵, F. Z. Qi¹, H. R. Qi⁶², M. Qi⁴³, S. Qian^{1,59}, W. B. Qian⁶⁵, C. F. Qiao⁶⁵, J. H. Qiao²⁰, J. J. Qin⁷⁴, J. L. Qin⁵⁶, L. Q. Qin¹⁴, L. Y. Qin^{73,59}, P. B. Qin⁷⁴, X. P. Qin^{12,g}, X. S. Qin⁵¹, Z. H. Qin^{1,59}, J. F. Qiu¹, Z. H. Qu⁷⁴,

J. Rademacker⁶⁴, C. F. Redmer³⁶, A. Rivetti^{76C}, M. Rojo^{76C}, G. Rong^{1,65}, S. S. Rong^{1,65}, F. Rosini^{29B,29C}, Ch. Rosner¹⁹, M. Q. Ruan^{1,59}, N. Salone⁴⁵, A. Sarantsev^{37,d}, Y. Schelhaas³⁶, K. Schoenning⁷⁷, M. Scodeggio^{30A}, K. Y. Shan^{12,g}, W. Shan²⁵, X. Y. Shan^{73,59}, Z. J. Shang^{39,k,l}, J. F. Shangguan¹⁷, L. G. Shao^{1,65}, M. Shao^{73,59}, C. P. Shen^{12,g}, H. F. Shen^{1,8}, W. H. Shen⁶⁵, X. Y. Shen^{1,65}, B. A. Shi⁶⁵, H. Shi^{73,59}, J. L. Shi^{12,g}, J. Y. Shi¹, S. Y. Shi⁷⁴, X. Shi^{1,59}, H. L. Song^{73,59}, J. J. Song²⁰, T. Z. Song⁶⁰, W. M. Song³⁵, Y. J. Song^{12,g}, Y. X. Song^{47,h,n}, S. Sosio^{76A,76C}, S. Spataro^{76A,76C}, F. Stieler³⁶, S. S. Su⁴¹, Y. J. Su⁶⁵, G. B. Sun⁷⁸, G. X. Sun¹, H. Sun⁶⁵, H. K. Sun¹, J. F. Sun²⁰, K. Sun⁶², L. Sun⁷⁸, S. S. Sun^{1,65}, T. Sun^{52,f}, Y. C. Sun⁷⁸, Y. H. Sun³¹, Y. J. Sun^{73,59}, Y. Z. Sun¹, Z. Q. Sun^{1,65}, Z. T. Sun⁵¹, C. J. Tang⁵⁵, G. Y. Tang¹, J. Tang⁶⁰, J. J. Tang^{73,59}, L. F. Tang⁴⁰, Y. A. Tang⁷⁸, L. Y. Tao⁷⁴, M. Tat⁷¹, J. X. Teng^{73,59}, J. Y. Tian^{73,59}, W. H. Tian⁶⁰, Y. Tian³², Z. F. Tian⁷⁸, I. Uman^{63B}, B. Wang¹, B. Wang⁶⁰, Bo Wang^{73,59}, C. Wang^{39,k,l}, C. Wang²⁰, Cong Wang²³, D. Y. Wang^{47,h}, H. J. Wang^{39,k,l}, J. J. Wang⁷⁸, K. Wang^{1,59}, L. L. Wang¹, L. W. Wang³⁵, M. Wang⁵¹, M. Wang^{73,59}, N. Y. Wang⁶⁵, S. Wang^{12,g}, T. Wang^{12,g}, T. J. Wang⁴⁴, W. Wang⁶⁰, W. Wang⁷⁴, W. P. Wang^{36,59,73,o}, X. Wang^{47,h}, X. F. Wang^{39,k,l}, X. J. Wang⁴⁰, X. L. Wang^{12,g}, X. N. Wang¹, Y. Wang⁶², Y. D. Wang⁴⁶, Y. F. Wang^{1,59,65}, Y. H. Wang^{39,k,l}, Y. J. Wang^{73,59}, Y. L. Wang²⁰, Y. N. Wang⁷⁸, Y. Q. Wang¹, Yaqian Wang¹⁸, Yi Wang⁶², Yuan Wang^{18,32}, Z. Wang^{1,59}, Z. L. Wang⁷⁴, Z. L. Wang², Z. Q. Wang^{12,g}, Z. Y. Wang^{1,65}, D. H. Wei¹⁴, H. R. Wei⁴⁴, F. Weidner⁷⁰, S. P. Wen¹, Y. R. Wen⁴⁰, U. Wiedner³, G. Wilkinson⁷¹, M. Wolke⁷⁷, C. Wu⁴⁰, J. F. Wu^{1,8}, L. H. Wu¹, L. J. Wu²⁰, L. J. Wu^{1,65}, Lianjie Wu²⁰, S. G. Wu^{1,65}, S. M. Wu⁶⁵, X. Wu^{12,g}, X. H. Wu³⁵, Y. J. Wu³², Z. Wu^{1,59}, L. Xia^{73,59}, X. M. Xian⁴⁰, B. H. Xiang^{1,65}, D. Xiao^{39,k,l}, G. Y. Xiao⁴³, H. Xiao⁷⁴, Y. L. Xiao^{12,g}, Z. J. Xiao⁴², C. Xie⁴³, K. J. Xie^{1,65}, X. H. Xie^{47,h}, Y. Xie⁵¹, Y. G. Xie^{1,59}, Y. H. Xie⁶, Z. P. Xie^{73,59}, T. Y. Xing^{1,65}, C. F. Xu^{1,65}, C. J. Xu⁶⁰, G. F. Xu¹, H. Y. Xu^{68,2}, H. Y. Xu², M. Xu^{73,59}, Q. J. Xu¹⁷, Q. N. Xu³¹, T. D. Xu⁷⁴, W. Xu¹, W. L. Xu⁶⁸, X. P. Xu⁵⁶, Y. Xu⁴¹, Y. Xu^{12,g}, Y. C. Xu⁷⁹, Z. S. Xu⁶⁵, F. Yan^{12,g}, H. Y. Yan⁴⁰, L. Yan^{12,g}, W. B. Yan^{73,59}, W. C. Yan⁸², W. H. Yan⁶, W. P. Yan²⁰, X. Q. Yan^{1,65}, H. J. Yang^{52,f}, H. L. Yang³⁵, H. X. Yang¹, J. H. Yang⁴³, R. J. Yang²⁰, T. Yang¹, Y. Yang^{12,g}, Y. F. Yang⁴⁴, Y. H. Yang⁴³, Y. Q. Yang⁹, Y. X. Yang^{1,65}, Y. Z. Yang²⁰, M. Ye^{1,59}, M. H. Ye⁸, Z. J. Ye^{57,j}, Junhao Yin⁴⁴, Z. Y. You⁶⁰, B. X. Yu^{1,59,65}, C. X. Yu⁴⁴, G. Yu¹³, J. S. Yu^{26,i}, L. Q. Yu^{12,g}, M. C. Yu⁴¹, T. Yu⁷⁴, X. D. Yu^{47,h}, Y. C. Yu⁸², C. Z. Yuan^{1,65}, H. Yuan^{1,65}, J. Yuan³⁵, J. Yuan⁴⁶, L. Yuan², S. C. Yuan^{1,65}, X. Q. Yuan¹, Y. Yuan^{1,65}, Z. Y. Yuan⁶⁰, C. X. Yue⁴⁰, Ying Yue²⁰, A. A. Zafar⁷⁵, S. H. Zeng^{64A,64B,64C,64D}, X. Zeng^{12,g}, Y. Zeng^{26,i}, Y. J. Zeng⁶⁰, Y. J. Zeng^{1,65}, X. Y. Zhai³⁵, Y. H. Zhan⁶⁰, A. Q. Zhang^{1,65}, B. L. Zhang^{1,65}, B. X. Zhang¹, D. H. Zhang⁴⁴, G. Y. Zhang^{1,65}, G. Y. Zhang²⁰, H. Zhang^{73,59}, H. Zhang⁸², H. C. Zhang^{1,59,65}, H. H. Zhang⁶⁰, H. Q. Zhang^{1,59,65}, H. R. Zhang^{73,59}, H. Y. Zhang^{1,59}, J. Zhang⁶⁰, J. Zhang⁸², J. J. Zhang⁵³, J. L. Zhang²¹, J. Q. Zhang⁴², J. S. Zhang^{12,g}, J. W. Zhang^{1,59,65}, J. X. Zhang^{39,k,l}, J. Y. Zhang¹, J. Z. Zhang^{1,65}, Jianyu Zhang⁶⁵, L. M. Zhang⁶², Lei Zhang⁴³, N. Zhang⁸², P. Zhang^{1,8}, Q. Zhang²⁰, Q. Y. Zhang³⁵, R. Y. Zhang^{39,k,l}, S. H. Zhang^{1,65}, Shulei Zhang^{26,i}, X. M. Zhang¹, X. Y. Zhang⁴¹, X. Y. Zhang⁵¹, Y. Zhang¹, Y. Zhang⁷⁴, Y. T. Zhang⁸², Y. H. Zhang^{1,59}, Y. M. Zhang⁴⁰, Y. P. Zhang^{73,59}, Z. D. Zhang¹, Z. H. Zhang¹, Z. L. Zhang³⁵, Z. L. Zhang⁵⁶, Z. X. Zhang²⁰, Z. Y. Zhang⁷⁸, Z. Y. Zhang⁴⁴, Z. Z. Zhang⁴⁶, Zh. Zh. Zhang²⁰, G. Zhao¹, J. Y. Zhao^{1,65}, J. Z. Zhao^{1,59}, L. Zhao^{73,59}, L. Zhao¹, M. G. Zhao⁴⁴, N. Zhao⁸⁰, R. P. Zhao⁶⁵, S. J. Zhao⁸², Y. B. Zhao^{1,59}, Y. L. Zhao⁵⁶, Y. X. Zhao^{32,65}, Z. G. Zhao^{73,59}, A. Zhemchugov^{37,b}, B. Zheng⁷⁴, B. M. Zheng³⁵, J. P. Zheng^{1,59}, W. J. Zheng^{1,65}, X. R. Zheng²⁰, Y. H. Zheng^{65,p}, B. Zhong⁴², C. Zhong²⁰, H. Zhou^{36,51,o}, J. Q. Zhou³⁵, J. Y. Zhou³⁵, S. Zhou⁶, X. Zhou⁷⁸, X. K. Zhou⁶, X. R. Zhou^{73,59}, X. Y. Zhou⁴⁰, Y. X. Zhou⁷⁹, Y. Z. Zhou^{12,g}, A. N. Zhu⁶⁵, J. Zhu⁴⁴, K. Zhu¹, K. J. Zhu^{1,59,65}, K. S. Zhu^{12,g}, L. Zhu³⁵, L. X. Zhu⁶⁵, S. H. Zhu⁷², T. J. Zhu^{12,g}, W. D. Zhu^{12,g}, W. D. Zhu⁴², W. J. Zhu¹, W. Z. Zhu²⁰, Y. C. Zhu^{73,59}, Z. A. Zhu^{1,65}, X. Y. Zhuang⁴⁴, J. H. Zou¹, and J. Zu^{73,59}

(BESIII Collaboration)

¹ Institute of High Energy Physics, Beijing 100049, People's Republic of China

² Beihang University, Beijing 100191, People's Republic of China

³ Bochum Ruhr-University, D-44780 Bochum, Germany

⁴ Budker Institute of Nuclear Physics SB RAS (BINP), Novosibirsk 630090, Russia

⁵ Carnegie Mellon University, Pittsburgh, Pennsylvania 15213, USA

⁶ Central China Normal University, Wuhan 430079, People's Republic of China

⁷ Central South University, Changsha 410083, People's Republic of China

⁸ China Center of Advanced Science and Technology, Beijing 100190, People's Republic of China

⁹ China University of Geosciences, Wuhan 430074, People's Republic of China

- ¹⁰ Chung-Ang University, Seoul, 06974, Republic of Korea
¹¹ COMSATS University Islamabad, Lahore Campus, Defence Road, Off Raiwind Road, 54000 Lahore, Pakistan
¹² Fudan University, Shanghai 200433, People's Republic of China
¹³ GSI Helmholtzcentre for Heavy Ion Research GmbH, D-64291 Darmstadt, Germany
¹⁴ Guangxi Normal University, Guilin 541004, People's Republic of China
¹⁵ Guangxi University, Nanning 530004, People's Republic of China
¹⁶ Guangxi University of Science and Technology, Liuzhou 545006, People's Republic of China
¹⁷ Hangzhou Normal University, Hangzhou 310036, People's Republic of China
¹⁸ Hebei University, Baoding 071002, People's Republic of China
¹⁹ Helmholtz Institute Mainz, Staudinger Weg 18, D-55099 Mainz, Germany
²⁰ Henan Normal University, Xinxiang 453007, People's Republic of China
²¹ Henan University, Kaifeng 475004, People's Republic of China
²² Henan University of Science and Technology, Luoyang 471003, People's Republic of China
²³ Henan University of Technology, Zhengzhou 450001, People's Republic of China
²⁴ Huangshan College, Huangshan 245000, People's Republic of China
²⁵ Hunan Normal University, Changsha 410081, People's Republic of China
²⁶ Hunan University, Changsha 410082, People's Republic of China
²⁷ Indian Institute of Technology Madras, Chennai 600036, India
²⁸ Indiana University, Bloomington, Indiana 47405, USA
²⁹ INFN Laboratori Nazionali di Frascati , (A)INFN Laboratori Nazionali di Frascati, I-00044, Frascati, Italy; (B)INFN Sezione di Perugia, I-06100, Perugia, Italy; (C)University of Perugia, I-06100, Perugia, Italy
³⁰ INFN Sezione di Ferrara, (A)INFN Sezione di Ferrara, I-44122, Ferrara, Italy; (B)University of Ferrara, I-44122, Ferrara, Italy
³¹ Inner Mongolia University, Hohhot 010021, People's Republic of China
³² Institute of Modern Physics, Lanzhou 730000, People's Republic of China
³³ Institute of Physics and Technology, Mongolian Academy of Sciences, Peace Avenue 54B, Ulaanbaatar 13330, Mongolia
³⁴ Instituto de Alta Investigación, Universidad de Tarapacá, Casilla 7D, Arica 1000000, Chile
³⁵ Jilin University, Changchun 130012, People's Republic of China
³⁶ Johannes Gutenberg University of Mainz, Johann-Joachim-Becher-Weg 45, D-55099 Mainz, Germany
³⁷ Joint Institute for Nuclear Research, 141980 Dubna, Moscow region, Russia
³⁸ Justus-Liebig-Universitaet Giessen, II. Physikalisches Institut, Heinrich-Buff-Ring 16, D-35392 Giessen, Germany
³⁹ Lanzhou University, Lanzhou 730000, People's Republic of China
⁴⁰ Liaoning Normal University, Dalian 116029, People's Republic of China
⁴¹ Liaoning University, Shenyang 110036, People's Republic of China
⁴² Nanjing Normal University, Nanjing 210023, People's Republic of China
⁴³ Nanjing University, Nanjing 210093, People's Republic of China
⁴⁴ Nankai University, Tianjin 300071, People's Republic of China
⁴⁵ National Centre for Nuclear Research, Warsaw 02-093, Poland
⁴⁶ North China Electric Power University, Beijing 102206, People's Republic of China
⁴⁷ Peking University, Beijing 100871, People's Republic of China
⁴⁸ Qufu Normal University, Qufu 273165, People's Republic of China
⁴⁹ Renmin University of China, Beijing 100872, People's Republic of China
⁵⁰ Shandong Normal University, Jinan 250014, People's Republic of China
⁵¹ Shandong University, Jinan 250100, People's Republic of China
⁵² Shanghai Jiao Tong University, Shanghai 200240, People's Republic of China
⁵³ Shanxi Normal University, Linfen 041004, People's Republic of China
⁵⁴ Shanxi University, Taiyuan 030006, People's Republic of China
⁵⁵ Sichuan University, Chengdu 610064, People's Republic of China
⁵⁶ Soochow University, Suzhou 215006, People's Republic of China
⁵⁷ South China Normal University, Guangzhou 510006, People's Republic of China

⁵⁸ *Southeast University, Nanjing 211100, People's Republic of China*

⁵⁹ *State Key Laboratory of Particle Detection and Electronics,
Beijing 100049, Hefei 230026, People's Republic of China*

⁶⁰ *Sun Yat-Sen University, Guangzhou 510275, People's Republic of China*

⁶¹ *Suranaree University of Technology, University Avenue 111, Nakhon Ratchasima 30000, Thailand*

⁶² *Tsinghua University, Beijing 100084, People's Republic of China*

⁶³ *Turkish Accelerator Center Particle Factory Group, (A)Istinye University, 34010, Istanbul,
Turkey; (B)Near East University, Nicosia, North Cyprus, 99138, Mersin 10, Turkey*

⁶⁴ *University of Bristol, H H Wills Physics Laboratory, Tyndall Avenue, Bristol, BS8 1TL, UK*

⁶⁵ *University of Chinese Academy of Sciences, Beijing 100049, People's Republic of China*

⁶⁶ *University of Groningen, NL-9747 AA Groningen, The Netherlands*

⁶⁷ *University of Hawaii, Honolulu, Hawaii 96822, USA*

⁶⁸ *University of Jinan, Jinan 250022, People's Republic of China*

⁶⁹ *University of Manchester, Oxford Road, Manchester, M13 9PL, United Kingdom*

⁷⁰ *University of Muenster, Wilhelm-Klemm-Strasse 9, 48149 Muenster, Germany*

⁷¹ *University of Oxford, Keble Road, Oxford OX13RH, United Kingdom*

⁷² *University of Science and Technology Liaoning, Anshan 114051, People's Republic of China*

⁷³ *University of Science and Technology of China, Hefei 230026, People's Republic of China*

⁷⁴ *University of South China, Hengyang 421001, People's Republic of China*

⁷⁵ *University of the Punjab, Lahore-54590, Pakistan*

⁷⁶ *University of Turin and INFN, (A)University of Turin, I-10125, Turin, Italy; (B)University
of Eastern Piedmont, I-15121, Alessandria, Italy; (C)INFN, I-10125, Turin, Italy*

⁷⁷ *Uppsala University, Box 516, SE-75120 Uppsala, Sweden*

⁷⁸ *Wuhan University, Wuhan 430072, People's Republic of China*

⁷⁹ *Yantai University, Yantai 264005, People's Republic of China*

⁸⁰ *Yunnan University, Kunming 650500, People's Republic of China*

⁸¹ *Zhejiang University, Hangzhou 310027, People's Republic of China*

⁸² *Zhengzhou University, Zhengzhou 450001, People's Republic of China*

^a Deceased

^b Also at the Moscow Institute of Physics and Technology, Moscow 141700, Russia

^c Also at the Novosibirsk State University, Novosibirsk, 630090, Russia

^d Also at the NRC "Kurchatov Institute", PNPI, 188300, Gatchina, Russia

^e Also at Goethe University Frankfurt, 60323 Frankfurt am Main, Germany

^f Also at Key Laboratory for Particle Physics, Astrophysics and Cosmology, Ministry
of Education; Shanghai Key Laboratory for Particle Physics and Cosmology; Institute
of Nuclear and Particle Physics, Shanghai 200240, People's Republic of China

^g Also at Key Laboratory of Nuclear Physics and Ion-beam Application (MOE) and
Institute of Modern Physics, Fudan University, Shanghai 200443, People's Republic of China

^h Also at State Key Laboratory of Nuclear Physics and Technology,
Peking University, Beijing 100871, People's Republic of China

ⁱ Also at School of Physics and Electronics, Hunan University, Changsha 410082, China

^j Also at Guangdong Provincial Key Laboratory of Nuclear Science, Institute
of Quantum Matter, South China Normal University, Guangzhou 510006, China

^k Also at MOE Frontiers Science Center for Rare Isotopes,
Lanzhou University, Lanzhou 730000, People's Republic of China

^l Also at Lanzhou Center for Theoretical Physics, Lanzhou University, Lanzhou 730000, People's Republic of China

^m Also at the Department of Mathematical Sciences, IBA, Karachi 75270, Pakistan

ⁿ Also at Ecole Polytechnique Federale de Lausanne (EPFL), CH-1015 Lausanne, Switzerland

^o Also at Helmholtz Institute Mainz, Staudinger Weg 18, D-55099 Mainz, Germany

^p Also at Hangzhou Institute for Advanced Study, University
of Chinese Academy of Sciences, Hangzhou 310024, China

Using e^+e^- collision data collected with the BESIII detector operating at the Beijing electron positron collider, the cross section of $e^+e^- \rightarrow \pi^+\pi^-h_c$ is measured at 59 points with center-of-mass energy \sqrt{s} ranging from 4.009 to 4.950 GeV with a total integrated luminosity of 22.2 fb^{-1} . The cross section between 4.3 and 4.45 GeV exhibits a plateau-like shape and drops sharply around 4.5 GeV, which cannot be described by two resonances only. Three coherent Breit-Wigner functions are used to parametrize the \sqrt{s} -dependent cross section line shape. The masses and widths are determined to be $M_1 = (4223.6^{+3.6+2.6}_{-3.7-2.9}) \text{ MeV}/c^2$, $\Gamma_1 = (58.5^{+10.8+6.7}_{-11.4-6.5}) \text{ MeV}$, $M_2 = (4327.4^{+20.1+10.7}_{-18.8-9.3}) \text{ MeV}/c^2$, $\Gamma_2 = (244.1^{+34.0+24.2}_{-27.1-18.3}) \text{ MeV}$, and $M_3 = (4467.4^{+7.2+3.2}_{-5.4-2.7}) \text{ MeV}/c^2$, and $\Gamma_3 = (62.8^{+19.2+9.9}_{-14.4-7.0}) \text{ MeV}$. The first uncertainties are statistical and the second are systematic. The inclusion of the relatively narrower third component proves crucial for reproducing the drop at around 4.5 GeV. The statistical significance of the three-resonance assumption over the two-resonance assumption is greater than 5σ .

The study of vector charmoniumlike states ($J^{PC} = 1^{--}$, known as Y states) has generated significant interest. The overpopulation of these Y states have led to exotic interpretations, including hybrid [1–5], tetraquark [6, 7], molecule [8–11] and hadrocharmonium states [12, 13], or kinematically induced peaks [14]. Meanwhile, the possibility that these states are excited charmonium states cannot be completely ruled out [15–17]. According to calculations based on an unquenched potential model, the $4S-3D$ and $5S-4D$ mixing charmonium states are predicted to lie between 4.2 and 4.5 GeV/c^2 , with widths ranging from 30 to 80 MeV [16], the $\psi(4230)$, $\psi(4360)$, $\psi(4415)$, and $\psi(4500)$ are assigned to be these states. Precise measurement of their properties is essential to unraveling their nature.

Among the processes in which the Y states are observed, those containing h_c in the final state are particularly interesting. This is because transitions between vector charmonium states and h_c are expected to be suppressed due to heavy quark spin symmetry, so a strong coupling is indicative of an exotic internal structure, such as hybrid configurations [18, 19]. The $e^+e^- \rightarrow \pi^+\pi^-h_c$ process was first observed by the CLEO Collaboration at a center-of-mass (c.m.) energy $\sqrt{s} = 4.17 \text{ GeV}$ [20]. Subsequently, the BESIII experiment studied the $e^+e^- \rightarrow \pi^+\pi^-h_c$ cross section with \sqrt{s} ranging from 3.896 to 4.600 GeV and observed the $Y(4220)$ and $Y(4390)$ [21]. Figure 1 presents the resonance parameters of $Y(4220)$ and $Y(4390)$ alongside those obtained from other processes [22–31], based on the BESIII scan samples. In the $Y(4390)$ region, resonances observed in different processes show significant variation in mass and width. At higher energies, new vector structures around 4.75 GeV have been reported by BESIII in $e^+e^- \rightarrow K\bar{K}J/\psi$ [30, 31] and $e^+e^- \rightarrow D_s^*D_s^*$ [32] processes. The decays of these higher Y states to h_c have not been investigated yet.

In this Letter, we report a measurement of the $e^+e^- \rightarrow \pi^+\pi^-h_c$ cross section at \sqrt{s} from 4.009 to 4.950 GeV. The data are collected with the BESIII detector [33] and include three sets: 19 energy points with large statistics [21] (referred to as XYZ-I), 25 energy points with lower statistics (referred to as XYZ-II), and 15 energy points, each with statistics of 8 pb^{-1} (referred to as R-scan).

The integrated luminosity of these samples is 22.2 fb^{-1} , determined from large-angle Bhabha events with an uncertainty of 1% [34, 35]. The c.m. energies for the XYZ-I and XYZ-II samples are determined from $e^+e^- \rightarrow \mu^+\mu^-$ or $e^+e^- \rightarrow \Lambda_c\bar{\Lambda}_c$ events [35–37], those for the R-scan samples are measured using multihadron final states.

In this study, the h_c is reconstructed via its electric-dipole transition $h_c \rightarrow \gamma\eta_c$ with $\eta_c \rightarrow X_i$, where X_i signifies 16 exclusive hadronic final states: $p\bar{p}$, $2(\pi^+\pi^-)$, $2(K^+K^-)$, $\pi^+\pi^-K^+K^-$, $\pi^+\pi^-p\bar{p}$, $3(\pi^+\pi^-)$, $2(\pi^+\pi^-)K^+K^-$, $K_S^0K^\pm\pi^\mp$, $K_S^0K^\pm\pi^\mp\pi^+\pi^-$, $K^+K^-\pi^0$, $p\bar{p}\pi^0$, $K^+K^-\eta$, $\pi^+\pi^-\eta$, $2(\pi^+\pi^-)\eta$, $\pi^+\pi^-\pi^0\pi^0$, and $2(\pi^+\pi^-\pi^0)$. The K_S^0 is reconstructed using its decay to $\pi^+\pi^-$, while π^0 and η are reconstructed through their $\gamma\gamma$ final state.

Monte Carlo (MC) samples are used to determine the detection efficiencies and to estimate the background contributions. They are produced with a GEANT4-based [38] simulation software package, which includes the geometric description of the BESIII detector and the detector response. The simulation models the beam energy spread and initial state radiation (ISR) in the e^+e^- annihilations with the generator KKMC [39]. The maximum energy of the ISR photon for the $e^+e^- \rightarrow \pi^+\pi^-h_c$ process corresponds to its kinematical threshold. The inclusive MC sample includes the production of open-charm processes, the ISR production of vector charmonium(-like) states, and the continuum processes. All particle decays are modeled with EVTGEN [40] using branching fractions either taken from Particle Data Group [41], when available, or otherwise estimated with LUNDCHARM [42]. Final state radiation from charged final state particles is incorporated using the PHOTOS package [43].

The event selection method is similar to the one used in Ref. [21]. However, the mass windows of π^0 , η , and η_c and the requirement of χ_{4C}^2 are re-optimized to enhance the signal-to-background ratio. For the $\eta_c \rightarrow \pi^+\pi^-\pi^0\pi^0$ and $\eta_c \rightarrow 2(\pi^+\pi^-\pi^0)$ modes, we further require $\chi_{4C}^2 < \chi_{4C,\pm\gamma}^2$, where χ_{4C}^2 is taken from a four-constraint (4C) kinematic fit of all selected final state particles with respect to the initial e^+e^- four momentum, and $\chi_{4C,\pm\gamma}^2$ is taken from the 4C kinematic fit that includes or excludes one photon. Figure 2 shows the invariant mass distribution of $\gamma\eta_c$ ($M_{\gamma\eta_c}$) in the η_c signal region for the sum

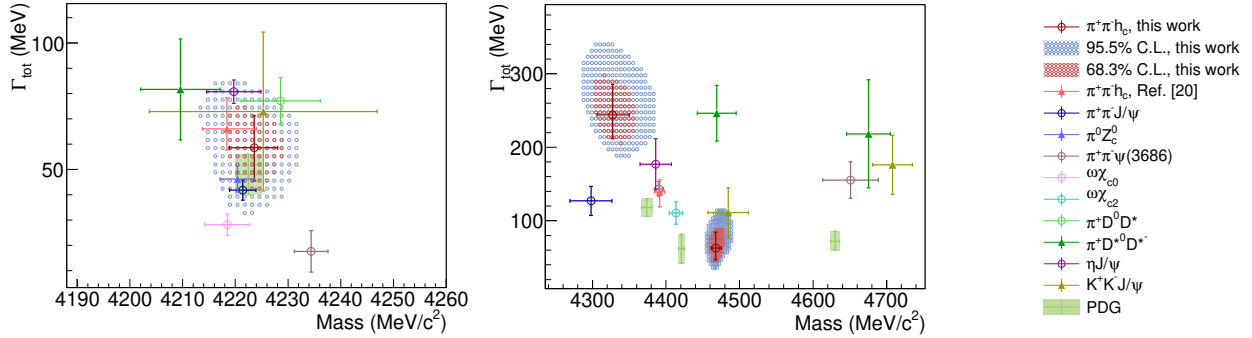


FIG. 1. Comparison of resonance parameters from hidden-charm or open-charm processes [21–31] (represented by dots with error bars in various colors), along with the parameters of $\psi(4230)$, $\psi(4360)$, $\psi(4415)$, and $\psi(4660)$ from PDG [41] (indicated by the green shaded square). The red and blue shaded regions represent the 68.3% and 95.5% CL regions determined in this work.

of the 16 decay channels at $\sqrt{s} = 4.236$ GeV. A clear $h_c \rightarrow \gamma\eta_c$ signal is observed. The background events are distributed linearly in the $M_{\gamma\eta_c}$ distribution, in agreement with the analysis of the inclusive MC sample.

The $e^+e^- \rightarrow \pi^+\pi^- h_c$ signal events yield is determined by performing an unbinned maximum likelihood fit to the $M_{\gamma\eta_c}$ spectrum. The signal contribution is modeled using the MC simulated shape, convolved with a Gaussian function which accounts for the resolution difference between data and the MC simulation. The background contribution is described by a linear function. For the XYZ-I data sample, a simultaneous fit to the 16 η_c decay modes is performed. The numbers of signal events in each mode are constrained according to the detection efficiencies and branching fractions. For the XYZ-II data sample, the $M_{\gamma\eta_c}$ spectra summed over the 16 η_c decay modes are fitted (referred to as the summed fit). Additionally, the parameters of the Gaussian function are fixed to the average values obtained from the fits to the XYZ-I data sample. The consistency between the results from the simultaneous fit and the summed fit is confirmed with the XYZ-I data sample. For the R-scan data sample, the summed fit method is used, with the background shape fixed according to that obtained from the summed fit to the XYZ-I and XYZ-II data sample in the range $4.3 \text{ GeV} < \sqrt{s} < 4.8 \text{ GeV}$.

The Born cross section σ^{Born} is calculated via:

$$\frac{N^{\text{obs}}}{\mathcal{L} \cdot (1 + \delta) \cdot (1/|1 - \Pi|^2) \cdot \mathcal{B}(h_c \rightarrow \gamma\eta_c) \cdot \sum_{i=1}^{16} \epsilon_i \mathcal{B}(\eta_c \rightarrow X_i)}, \quad (1)$$

where N^{obs} , \mathcal{L} , $(1 + \delta)$, and $(1/|1 - \Pi|^2)$ are the signal yields, the integrated luminosity, the ISR correction factor, and the vacuum polarization correction factor, respectively. For the i th η_c decay mode, ϵ_i represents the detection efficiency, and $\mathcal{B}(\eta_c \rightarrow X_i)$ denotes the branching fraction. The branching fractions of $h_c \rightarrow \gamma\eta_c$ and the η_c decays are taken from previous BESIII measurements [44, 45]. The cross section is obtained through

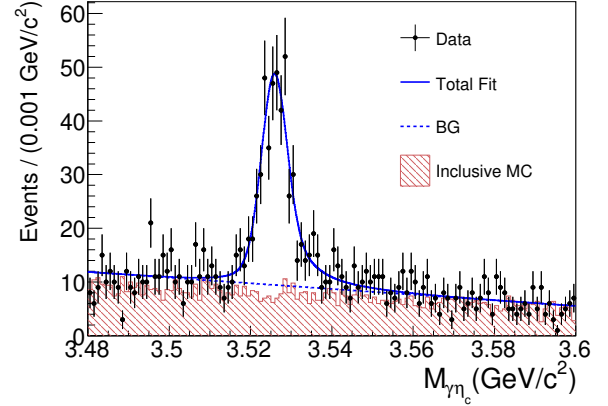


FIG. 2. The $M_{\gamma\eta_c}$ distribution in the η_c signal region at $\sqrt{s} = 4.236$ GeV. Dots with error bars are the data, the solid curve is the best fit result, and the dashed curve represents the background contribution.

an iterative procedure, since both the ISR factor and the detection efficiency depend on the cross section line shape [46]. The procedure adopts the dressed cross section as its input, which is the product of the Born cross section and the vacuum polarization correction factor. The dressed cross sections are shown in Fig. 3 and summarized in the Supplemental Material [47], together with all the inputs used in the calculation.

The \sqrt{s} -dependent dressed cross section is fitted using a maximum likelihood method to investigate the vector resonance structures. The best fit is achieved with a model incorporating three coherent Breit-Wigner (BW) functions (the baseline model), which is written as

$$|BW_1(\sqrt{s}) + e^{i\phi_2} BW_2(\sqrt{s}) + e^{i\phi_3} BW_3(\sqrt{s})|^2. \quad (2)$$

Here, BW_k with $k = 1, 2$ or 3 is used to describe the

resonance, defined as

$$\frac{M_k}{\sqrt{s}} \cdot \frac{\sqrt{12\pi(\Gamma_{ee}\mathcal{B}(R_k \rightarrow \pi^+\pi^- h_c))_k \Gamma_k}}{s - M_k^2 + iM_k\Gamma_k} \cdot \sqrt{\frac{PS(\sqrt{s})}{PS(M_k)}}. \quad (3)$$

In the fit, the mass M_k , the total width Γ_k , the product of the electromagnetic width and the branching fraction $[\Gamma_{ee}\mathcal{B}(R_k \rightarrow \pi^+\pi^- h_c)]_k$, and the relative phase ϕ_k are free parameters.

In the baseline model, four solutions with two sets of parameters are found in accordance with expectations [48]. The fit results are shown in Fig. 3, and the resonance parameters are listed in Table I. The mass versus width plots for the three resonance structures, along with the 68.3% and 95.5% confidence level (CL) contours are shown in Fig. 1, together with the resonance parameters of vector charmonium(-like) states observed in other processes. The parameters of the first resonance are consistent with those reported for $Y(4220)$ by BESIII. However, the mass and width of the second resonance [$M = (4327.4^{+20.1}_{-18.8}) \text{ MeV}/c^2$, $\Gamma_{\text{tot}} = (244.1^{+34.0}_{-27.1}) \text{ MeV}$] are found to be 60 MeV/ c^2 lower and 100 MeV wider compared to the reported values for $Y(4390)$ from previous study of the same process [$M = (4391.6 \pm 6.3 \pm 1.0) \text{ MeV}/c^2$, $\Gamma_{\text{tot}} = (139.5 \pm 16.1 \pm 0.6) \text{ MeV}$] [21, 47]. This discrepancy arises from the inclusion of a third resonance in this work. The model using two coherent BW functions cannot describe the dip in the cross section at $\sqrt{s} = 4.498 \text{ GeV}$ [47]. The fit quality is calculated to be $\chi^2/ndf = 77.9/66$ in the two-resonance fit and 41.9/70 when the third resonance is added. Result of the two-resonance fit is shown in Supplemental Material [47]. The statistical significance of the third resonance is 5.4σ , estimated by utilizing the changes in likelihood values ($\delta(-2\ln L) = 38.8$) and the number of degrees of freedom ($\delta(ndf) = 4$).

Several parametrization models are tested. Adding one resonance with free parameters or a phase space term [$PS(\sqrt{s})/s^n$] to the baseline model slightly improves the fit quality. The statistical significance of this fourth resonance (or phase space term) is 0.7σ (0.1σ), where $PS(\sqrt{s})$ is the three-body phase space factor. The model used in Ref. [14] is also tested, yielding a nonconvergent fit. The cross section is then updated using the baseline model as input cross section line shape and iterated until convergence.

Systematic uncertainties in the cross section measurement come mainly from the integrated luminosity, the statistical uncertainties of the c.m. energy for the R-scan data sample, the input cross section line shape, the branching fractions, the detection efficiency, and the determination of N^{obs} . The uncertainty of the integrated luminosity is 1% [34, 35]. The effect from the statistical uncertainties of the c.m. energy for the R-scan data sample is estimated by shifting \sqrt{s} by $\pm 1 \text{ MeV}$. The uncertainty from the parametrization of the cross section

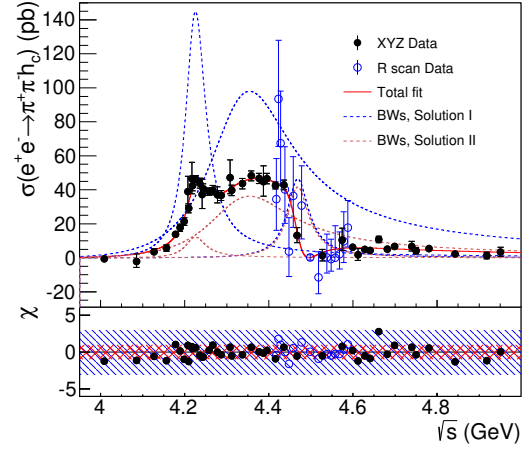


FIG. 3. Fit to the dressed cross section for the two solutions for $e^+e^- \rightarrow \pi^+\pi^- h_c$ with the baseline model (the red curve). The blue and red dashed curves are contributions from the three structures. The dots with error bars are the converged cross section. The bottom panel shows the χ values, in which the red and blue shadings represent ± 1 and ± 3 , respectively.

line shape is estimated by adding a phase space term to Eq. 2. The difference is 1%, and is taken as the uncertainty. The uncertainty of the cross section is reflected by the uncertainty of the parameters in the formula used to describe the cross section line shape. This is estimated by sampling these parameters according to the covariance matrix and recalculating the ISR factor, and the standard deviation of the resultant distribution is taken as the systematic uncertainty. The combined branching fractions $\mathcal{B}(h_c \rightarrow \gamma\eta_c) \cdot \mathcal{B}(\eta_c \rightarrow X_i)$ are taken from Ref. [44], updated with the latest measurement of $\psi(3686) \rightarrow \pi^0 h_c$ from BESIII [45], giving an uncertainty of 9.7%.

The uncertainty related to the detection efficiency contains the tracking efficiency, photon reconstruction, K_S^0 reconstruction, π^0/η mass window, η_c mass window, χ^2_{4C} requirement, and intermediate states in πh_c and $\pi^+\pi^-$ system. The first four terms are not added in this study since they are included in the branching fraction of η_c . The uncertainties of the two additional pion tracks accompanying the h_c are also included (1% per track). The uncertainties from the mass, width [41], and line shape of η_c [49] used in MC simulations are estimated by varying them within uncertainties or adding the missing terms and check the difference in detection efficiencies, which are 1.1% for the η_c parameters and 0.2% for the line shape. The uncertainty from the applied requirement on the χ^2_{4C} value is estimated by correcting the helix parameter of charged particles to match the resolution in data [50]. The uncertainty from the requirement of $\chi^2_{4C} < \chi^2_{4C,\pm\gamma}$ is estimated by removing this requirement and repeating the analysis. The systematic uncer-

TABLE I. The fit results from the baseline model. The first uncertainty is statistical and second systematic. The numbers in brackets are from the second solution with equal fit quality.

Parameter	R_1	R_2	R_3
M (MeV/c ²)	$4223.6^{+3.6+2.6}_{-3.7-2.9}$	$4327.4^{+20.1+10.7}_{-18.8-9.3}$	$4467.4^{+7.2+3.2}_{-5.4-2.7}$
Γ (MeV)	$58.5^{+10.8+6.7}_{-11.4-6.5}$	$244.1^{+34.0+24.2}_{-27.1-18.3}$	$62.8^{+19.2+9.9}_{-14.4-7.0}$
$\Gamma_{ee} \cdot \mathcal{B}(R \rightarrow \pi^+\pi^- h_c)$ (eV)	$10.2^{+1.2+1.4}_{-1.5-1.4} (0.9^{+0.4+0.3}_{-0.4-0.2})$	$29.1^{+5.7+4.4}_{-3.9-3.4} (10.8^{+2.5+1.9}_{-1.8-1.5})$	$3.9^{+3.5+1.7}_{-1.7-0.5} (3.5^{+3.0+1.5}_{-1.6-0.7})$
ϕ (rad)	...	$3.6^{+0.1+0.1}_{-0.1-0.1} (0.7^{+0.3+0.2}_{-0.3-0.2})$	$0.7^{+0.3+0.1}_{-0.3-0.2} (-2.2^{+0.3+0.2}_{-0.3-0.1})$

tainties for the two aforementioned terms are 2.1% and 2.3%, respectively. The uncertainty from the intermediate states in πh_c and $\pi^+\pi^-$ system is estimated by reweighting the MC simulation using a Dalitz plot obtained from data, and is 8.0%, 12.5%, and 3.5% for data the samples at $\sqrt{s} = 4.189$ GeV, $\sqrt{s} = 4.199$ GeV, and the other c.m. energies.

The uncertainties in the determination of N^{obs} are estimated by varying the fit conditions and observing the resulting changes in the cross section results. Uncertainties from the fixed parameters in the fit, including the mass resolution difference between data and MC simulation for XYZ-II and R-scan data sample, as well as the background shape for R-scan data sample, are estimated by adjusting each parameter by 1 standard deviation. To access the uncertainty from the background shape, the linear function is replaced with a second order Chebyshev function, the impact on the results is negligible. The uncertainty from the fit range is tested by modifying the nominal fit range by ± 5 and ± 10 MeV/c² and examining the uncorrelated uncertainty as outlined in [51, 52], which is found negligible. The total systematic uncertainty in the $e^+e^- \rightarrow \pi^+\pi^- h_c$ cross section measurement, listed in Supplemental Material [47], is determined by assuming these sources as independent.

The systematic uncertainties for the parameters of the resonance structures are summarized in Table II. They primarily arise from the systematic and statistical uncertainties of the c.m. energy, the beam energy spread, the systematic uncertainty of the cross section, and the choice of the parametrization model. The impact of the systematic uncertainty in the c.m. energy measurement is 0.6 MeV [35–37] and only affects the mass measurements. The effect from the statistical uncertainty in c.m. energy measurement for the R-scan data sample is estimated by randomly modifying the corresponding \sqrt{s} values according to a Gaussian function with mean 0 and standard deviation 1 MeV, and reevaluating the resonance parameters.

The uncertainties from cross section measurement are divided into two classes. “Cross section I” relates to the uncorrelated terms, including the mass resolution difference between data and MC simulation, fixed background shape for the R-scan sample, ISR factor, and uncorrelated systematic uncertainty terms in the detection efficiency (the requirement of $\chi^2_{4C} < \chi^2_{4C,\pm\gamma}$ and the in-

termediate states in $\pi\pi h_c$ system). They are considered by adding these terms to the statistical uncertainty. The systematic uncertainty for each parameter is calculated with $\sqrt{\delta_{w/}^2 - \delta_{w/o}^2}$, where $\delta_{w/}$ and $\delta_{w/o}$ are the uncertainties with and without the systematic terms included. “Cross section II” represents the correlated terms common to all data samples, estimated to be 10.2%. The uncertainty from the parameterization model is estimated by adding a phase space term to the baseline model. The cross section is obtained through an iterative procedure, since both the ISR factor and the detection efficiency depend on the cross section line shape [46]. The systematic uncertainty due to iteration stability is the maximum difference (1.0%) across all energy points between the final two iterations. The uncertainty from the beam energy spread is estimated by convolving a Gaussian function (with the standard deviation provided by the beam energy measurement system [53]) to the fit formula.

In summary, we measure the $e^+e^- \rightarrow \pi^+\pi^- h_c$ cross section at 59 energy points from $\sqrt{s} = 4.009$ to 4.951 GeV. The cross section between 4.3 and 4.45 GeV exhibits a plateau-like shape and has a dip at 4.5 GeV. The best description of the cross section line shape is achieved by the coherent sum of three BW functions. The significance of the third resonance is larger than 5σ . No obvious resonance structure is observed at around $\psi(4660)$, which is in tension with the theoretical prediction in a hidden charm P -wave tetraquark model [54].

The mass and width of the first resonance are consistent with the $\psi(4230)$ [41] and the observation in a previous study of the same process [21]. The mass of the second resonance is consistent with the $\psi(4360)$ [41], but the obtained width is about 100 MeV broader. It is noteworthy that the mass of the second resonance is much closer to the resonance observed in $e^+e^- \rightarrow \pi^+\pi^- J/\psi$ [22], with respect to the previous study [21]. The parameters of the third resonance are consistent with the $\psi(4500)$ found in K^+K^-J/ψ [30, 31], whereas the mass is 40 MeV higher than the $\psi(4415)$.

The model proposed in Ref. [14] cannot describe the cross section line shape, where the structure around 4.39 GeV is attributed to the interference between $\psi(4160)$ and $\psi(4415)$. Subsequent studies predict two pairs of $S - D$ mixing vector charmonium states [16]. The masses of R_1 and R_2 align with the $4S - 3D$ mixing

TABLE II. The systematic uncertainty in the measurement of resonance parameters of the Y states. The numbers in brackets indicate uncertainty of the second solution. Syst. and stat. refer to systematic and statistical uncertainties of the c.m. energy measurement, respectively.

Sources	R_1			R_2				R_3			
	M (MeV/c 2)	Γ_{tot} (MeV)	$\Gamma_{ee} \cdot \mathcal{B}$ (%)	M (MeV/c 2)	Γ_{tot} (MeV)	$\Gamma_{ee} \cdot \mathcal{B}$ (%)	ϕ (rad)	M (MeV/c 2)	Γ_{tot} (MeV)	$\Gamma_{ee} \cdot \mathcal{B}$ (%)	ϕ (rad)
c.m. energy (syst.)	0.6	0.6	0.6
c.m. energy (stat.)	0.0	0.1	0.0 (0.3)	0.1	0.4	0.2 (0.2)	0.0 (0.0)	0.1	0.3	0.8 (0.6)	0.0 (0.0)
Cross section I	+2.5 -2.8	+6.4 -6.1	+8.1 (28.2) -8.0 (17.9)	+10.6 -9.1	+20.2 -13.1	+10.3 (11.1) -5.7 (4.3)	+0.1 (0.2) -0.1 (0.2)	+2.9 -2.4	+8.9 -6.1	+37.8 (38.4) -4.5 (14.6)	+0.1 (0.2) -0.2 (0.1)
Cross section II	10.2	10.2	10.2	...
Parametrization	0.4	1.8	3.2 (9.4)	1.1	12.3	0.7 (8.6)	0.0 (0.0)	0.8	2.4	3.9 (4.9)	0.1 (0.0)
Energy spread	+0.4 -0.3	+1.1 -1.3	+0.8 (3.3) -1.8 (3.4)	+0.7 -1.1	+5.1 -3.5	+4.0 (4.7) -1.1 (1.8)	+0.0 (0.0) -0.0 (0.0)	+0.9 -0.7	+3.6 -2.3	+19.3 (17.7) -1.7 (1.2)	+0.0 (0.0) -0.0 (0.0)
Total	+2.6 -2.9	+6.7 -6.5	+13.5 (31.6) -13.5 (22.9)	+10.7 -9.3	+24.2 -18.3	+15.1 (18.0) -11.8 (14.2)	+0.1 (0.2) -0.1 (0.2)	+3.2 -2.7	+9.9 -7.0	+43.8 (43.8) -12.0 (18.6)	+0.1 (0.2) -0.2 (0.1)

model; however, the width of R_2 significantly exceeds the predicted limit of $\Gamma_2 \leq 80$ MeV. While R_3 could be one of the $5S - 4D$ states, its expected partner is not seen. Additionally, the mass of R_2 and R_3 are also close to that of $\psi(3D)$, yet the large width of R_2 is incompatible with the model [15, 17]. Notably, the mass and width of R_3 are consistent with a hybrid state prediction [4].

Reference [55] suggests $\mathcal{O}(10^2)$ eV $\lesssim \Gamma_{ee}^{Y(4260)} \lesssim \mathcal{O}(10^3)$ eV. Assuming $\Gamma_{ee}^{R_1, R_2} \in (10^2, 10^3)$ eV, we determine $\Gamma_{\pi^+ \pi^- h_c}^{R_1} \in (0.05, 0.5)$ MeV or (0.6, 6.0) MeV and $\Gamma_{\pi^+ \pi^- h_c}^{R_2} \in (2.6, 26.4)$ MeV or (7.1, 71.0) MeV for the two solutions. $\Gamma_{\pi^+ \pi^- h_c}^{R_1}$ lies within the upper limit $\Gamma_{\pi^+ \pi^- h_c}^{\psi(4230)} < 1.26$ MeV set by a molecular model calculation[8]. The $\Gamma_{\pi^+ \pi^- h_c}^{R_1}$ is smaller than hybrid configuration predictions, which are $\Gamma_{h_c + l.h.}^{\psi(4230)} = 17(15)$ and $\Gamma_{h_c + l.h.}^{\psi(4360)} = 14(12)$ MeV, where $l.h.$ stands for light hadrons [5]. However, the model cannot be excluded due to large uncertainties of the theoretical result.

Acknowledgments—The BESIII Collaboration thanks the staff of BEPCII [56] and the IHEP computing center for their strong support. This work is supported in part by National Key R&D Program of China under Contracts No. 2020YFA0406300, No. 2020YFA0406400, No. 2023YFA1606000, No. 2023YFA1606704; National Natural Science Foundation of China (NSFC) under Contracts No. 12375070, No. 11635010, No. 11935015, No. 11935016, No. 11935018, No. 12025502, No. 12035009, No. 12035013, No. 12061131003, No. 12192260, No. 12192261, No. 12192262, No. 12192263, No. 12192264, No. 12192265, No. 12221005, No. 12225509, No. 12235017, No. 12361141819; the Chinese Academy of Sciences (CAS) Large-Scale Scientific Facility Program; CAS under Contract No. YSBR-101; Joint Large-Scale Scientific Facility Funds of the NSFC and CAS under Contract No.U2032108; Shanghai Leading Talent Program of Eastern Talent Plan under Contract No. JLH5913002; 100 Talents Program of CAS; The Institute of Nuclear and Particle Physics (INPAC) and Shanghai Key Laboratory for Part-

ticle Physics and Cosmology; Agencia Nacional de Investigación y Desarrollo de Chile (ANID), Chile under Contract No. ANID PIA/APOYO AFB230003; German Research Foundation DFG under Contract No. FOR5327; Istituto Nazionale di Fisica Nucleare, Italy; Knut and Alice Wallenberg Foundation under Contracts No. 2021.0174, No. 2021.0299; Ministry of Development of Turkey under Contract No. DPT2006K-120470; National Research Foundation of Korea under Contract No. NRF-2022R1A2C1092335; National Science and Technology fund of Mongolia; National Science Research and Innovation Fund (NSRF) via the Program Management Unit for Human Resources & Institutional Development, Research and Innovation of Thailand under Contract No. B50G670107; Polish National Science Centre under Contract No. 2024/53/B/ST2/00975; Swedish Research Council under Contract No. 2019.04595; U. S. Department of Energy under Contract No. DE-FG02-05ER41374

Data availability—The data that support the findings of this article are openly available [57].

-
- [1] S. L. Zhu, Phys. Lett. B **625**, 212 (2005).
 - [2] F. E. Close and P. R. Page, Phys. Lett. B **628**, 215 (2005).
 - [3] E. Kou and O. Pene, Phys. Lett. B **631**, 164 (2005).
 - [4] N. Brambilla, W. K. Lai, A. Mohapatra, and A. Vairo, Phys. Rev. D **107**, 054034 (2023).
 - [5] R. Oncala and J. Soto, Phys. Rev. D **96**, 014004 (2017).
 - [6] L. Maiani, F. Piccinini, A. D. Polosa, and V. Riquer, Phys. Rev. D **89**, 114010 (2014).
 - [7] Z. G. Wang, Nucl. Phys. **B973**, 115592 (2021).
 - [8] D. Y. Chen, C. J. Xiao, and J. He, Phys. Rev. D **96**, 054017 (2017).
 - [9] G. J. Ding, Phys. Rev. D **79**, 014001 (2009).
 - [10] Q. Wang, C. Hanhart, and Q. Zhao, Phys. Rev. Lett. **111**, 132003 (2013).
 - [11] M. Cleven, Q. Wang, F. K. Guo, C. Hanhart, Ulf-G. Meißner, and Q. Zhao, Phys. Rev. D **90**, 074039 (2014).

- [12] X. Li and M. B. Voloshin, Mod. Phys. Lett. A **29**, 1450060 (2014).
- [13] S. Dubynskiy and M. B. Voloshin, Phys. Lett. B **666**, 344 (2008).
- [14] D. Y. Chen, X. Liu, and T. Matsuki, Eur. Phys. J. C **78**, 136 (2018).
- [15] D. Y. Chen, C. Q. Pang, J. He, and Z. Y. Zhou, Phys. Rev. D **100**, 074016 (2019).
- [16] J. Z. Wang, D. Y. Chen, X. Liu, and T. Matsuki, Phys. Rev. D **99**, 114003 (2019).
- [17] S. Godfrey and N. Isgur, Phys. Rev. D **32**, 189 (1985).
- [18] N. Brambilla, S. Eidelman, C. Hanhart, A. Nefediev, C. P. Shen, C. E. Thomas, A. Vairo, and C. Z. Yuan, Phys. Rep. **873**, 1 (2020).
- [19] Y. Chen, W. F. Chiu, M. Gong, L. C. Gui, and Z. Liu, Chin. Phys. C **40**, 081002 (2016).
- [20] T. K. Pedlar *et al.* (CLEO Collaboration), Phys. Rev. Lett. **107**, 041803 (2011).
- [21] M. Ablikim *et al.* (BESIII Collaboration), Phys. Rev. Lett. **118** 092002 (2017).
- [22] M. Ablikim *et al.* (BESIII Collaboration), Phys. Rev. D **106**, 072001 (2022); Phys. Rev. Lett. **118**, 092001 (2017).
- [23] M. Ablikim *et al.* (BESIII Collaboration), Phys. Rev. D **102**, 012009 (2020).
- [24] M. Ablikim *et al.* (BESIII Collaboration), Phys. Rev. D **104**, 052012 (2021).
- [25] M. Ablikim *et al.* (BESIII Collaboration), Phys. Rev. D **99**, 091103 (2019).
- [26] M. Ablikim *et al.* (BESIII Collaboration), Phys. Rev. Lett. **132**, 161901 (2024).
- [27] M. Ablikim *et al.* (BESIII Collaboration), Phys. Rev. Lett. **122**, 102002 (2019).
- [28] M. Ablikim *et al.* (BESIII Collaboration), Phys. Rev. Lett. **130**, 121901 (2023).
- [29] M. Ablikim *et al.* (BESIII Collaboration), Phys. Rev. D **102**, 031101 (2020).
- [30] M. Ablikim *et al.* (BESIII Collaboration), Chin. Phys. C **46**, 111002 (2022).
- [31] M. Ablikim *et al.* (BESIII Collaboration), Phys. Rev. Lett. **131**, 211902 (2023).
- [32] M. Ablikim *et al.* (BESIII Collaboration), Phys. Rev. Lett. **131**, 151903 (2023).
- [33] M. Ablikim *et al.* (BESIII Collaboration), Instrum. Methods Phys. Res., Sect. A **614**, 345 (2010).
- [34] M. Ablikim *et al.* (BESIII Collaboration), Chin. Phys. C **46**, 113002 (2022).
- [35] M. Ablikim *et al.* (BESIII Collaboration), Chin. Phys. C **46**, 113003 (2022).
- [36] M. Ablikim *et al.* (BESIII Collaboration), Chin. Phys. C **40**, 063001 (2016).
- [37] M. Ablikim *et al.* (BESIII Collaboration), Chin. Phys. C **45**, 103001 (2021).
- [38] S. Agostinelli *et al.* (GEANT4 Collaboration), Nucl. Instrum. Methods Phys. Res., Sect. A **506**, 250 (2003).
- [39] S. Jadach, B. F. L. Ward, and Z. Was, Phys. Rev. D **63**, 113009 (2001); Comput. Phys. Commun. **130**, 260 (2000).
- [40] D. J. Lange, Instrum. Methods Phys. Res., Sect. A **462**, 152 (2001); R. G. Ping, Chin. Phys. C **32**, 599 (2008).
- [41] S. Navas *et al.* (Particle Data Group), Phys. Rev. D **110**, 030001 (2024).
- [42] J. C. Chen, G. S. Huang, X. R. Qi, D. H. Zhang, and Y. S. Zhu, Phys. Rev. D **62**, 034003 (2000); R. L. Yang, R. G. Ping, and H. Chen, Chin. Phys. Lett. **31**, 061301 (2014).
- [43] E. Barberio, B. van Eijk, and Z. Was, Comput. Phys. Commun. **66**, 115 (1991).
- [44] M. Ablikim *et al.* (BESIII Collaboration), Phys. Rev. D **86**, 092009 (2012).
- [45] M. Ablikim *et al.* (BESIII Collaboration), Phys. Rev. D **106**, 072007 (2022).
- [46] W. Y. Sun, T. Liu, M. Q. Jing, L. L. Wang, B. Zhong, and W. M. Song, Front. Phys. **16**, 64501 (2021).
- [47] See Supplemental Material at 10.1103/PhysRevLett.135.071901 for the fit result with two coherent Breit-Wigner functions, and a summary of the signal yields, luminosity, the dressed cross section at each energy point.
- [48] Y. Bai and D. Y. Chen, Phys. Rev. D **99**, 072007 (2019).
- [49] V. V. Anashin, *et al.* Int. J. Mod. Phys. Conf. Ser. **02**, 188 (2011).
- [50] M. Ablikim *et al.* (BESIII Collaboration), Phys. Rev. D **87**, 012002 (2013).
- [51] R. Barlow, arXiv:hep-ex/0207026.
- [52] Wanke, R. *Data Analysis in High Energy Physics: A Practical Guide to Statistical Methods*. edited by O. Behnke, K. Kroninger, G.P. Schott, and T. Schorner-Sadenius, (Wiley-VCH Verlag GmbH & Co. KGaA, New York, 2013).
- [53] E. V. Abakumova, M. N. Achasov, V. E. Blinov, X. Cai, H. Y. Dong, C. D. Fu, F. A. Harris, V. V. Kaminsky, A. A. Krasnov, and Q. Liu, *et al.* Nucl. Instrum. Methods Phys. Res., Sect. A **659**, 21 (2011).
- [54] A. Ali, L. Maiani, A. V. Borisov, I. Ahmed, M. Jamil Aslam, A. Y. Parkhomenko, A. D. Polosa, and A. Rehman, Eur. Phys. J. C **78**, 29 (2018).
- [55] Q. F. Cao, H. R. Qi, G. Y. Tang, Y. F. Xue, and H. Q. Zheng, Eur. Phys. J. C **81**, 83 (2021).
- [56] <https://cstr.cn/31109.02.BEPC>
- [57] BESIII Collaboration, Observation of three resonant structures in the cross section of $e^+e^- \rightarrow \pi^+\pi^-h_c$, HEP-Data (collection) (2025), doi:10.17182/hepdata.160247.

Supplemental Material for “Observation of Three Resonant Structures in the Cross Section of $e^+e^- \rightarrow \pi^+\pi^- h_c$ ”

M. Ablikim¹, M. N. Achasov^{4,c}, P. Ad larson⁷⁷, X. C. Ai⁸², R. Aliberti³⁶, A. Amoroso^{76A,76C}, Q. An^{73,59,a}, Y. Bai⁵⁸, O. Bakina³⁷, Y. Ban^{47,h}, H.-R. Bao⁶⁵, V. Batozskaya^{1,45}, K. Begzsuren³³, N. Berger³⁶, M. Berlowski⁴⁵, M. Bertani^{29A}, D. Bettone^{30A}, F. Bianchi^{76A,76C}, E. Bianco^{76A,76C}, A. Bortone^{76A,76C}, I. Boyko³⁷, R. A. Briere⁵, A. Brueggemann⁷⁰, H. Cai⁷⁸, M. H. Cai^{39,k,l}, X. Cai^{1,59}, A. Calcaterra^{29A}, G. F. Cao^{1,65}, N. Cao^{1,65}, S. A. Cetin^{63A}, X. Y. Chai^{47,h}, J. F. Chang^{1,59}, G. R. Che⁴⁴, Y. Z. Che^{1,59,65}, C. H. Chen⁹, Chao Chen⁵⁶, G. Chen¹, H. S. Chen^{1,65}, H. Y. Chen²¹, M. L. Chen^{1,59,65}, S. J. Chen⁴³, S. L. Chen⁴⁶, S. M. Chen⁶², T. Chen^{1,65}, X. R. Chen^{32,65}, X. T. Chen^{1,65}, X. Y. Chen^{12,g}, Y. B. Chen^{1,59}, Y. Q. Chen¹⁶, Y. Q. Chen³⁵, Z. J. Chen^{26,i}, Z. K. Chen⁶⁰, S. K. Choi¹⁰, X. Chu^{12,g}, G. Cibinetto^{30A}, F. Cossio^{76C}, J. Cottee-Meldrum⁶⁴, J. J. Cui⁵¹, H. L. Dai^{1,59}, J. P. Dai⁸⁰, A. Dbeysi¹⁹, R. E. de Boer³, D. Dedovich³⁷, C. Q. Deng⁷⁴, Z. Y. Deng¹, A. Denig³⁶, I. Denysenko³⁷, M. Destefanis^{76A,76C}, F. De Mori^{76A,76C}, B. Ding^{68,1}, X. X. Ding^{47,h}, Y. Ding³⁵, Y. Ding⁴¹, Y. X. Ding³¹, J. Dong^{1,59}, L. Y. Dong^{1,65}, M. Y. Dong^{1,59,65}, X. Dong⁷⁸, M. C. Du¹, S. X. Du⁸², S. X. Du^{12,g}, Y. Y. Duan⁵⁶, P. Egorov^{37,b}, G. F. Fan⁴³, J. J. Fan²⁰, Y. H. Fan⁴⁶, J. Fang⁶⁰, J. Fang^{1,59}, S. S. Fang^{1,65}, W. X. Fang¹, Y. Q. Fang^{1,59}, R. Farinelli^{30A}, L. Fava^{76B,76C}, F. Feldbauer³, G. Felici^{29A}, C. Q. Feng^{73,59}, J. H. Feng¹⁶, L. Feng^{39,k,l}, Q. X. Feng^{39,k,l}, Y. T. Feng^{73,59}, M. Fritsch³, C. D. Fu¹, J. L. Fu⁶⁵, Y. W. Fu^{1,65}, H. Gao⁶⁵, X. B. Gao⁴², Y. Gao^{73,59}, Y. N. Gao^{47,h}, Y. N. Gao²⁰, Y. Y. Gao³¹, S. Garbolino^{76C}, I. Garzia^{30A,30B}, P. T. Ge²⁰, Z. W. Ge⁴³, C. Geng⁶⁰, E. M. Gersabeck⁶⁹, A. Gilman⁷¹, K. Goetzen¹³, J. D. Gong³⁵, L. Gong⁴¹, W. X. Gong^{1,59}, W. Gradl³⁶, S. Gramigna^{30A,30B}, M. Greco^{76A,76C}, M. H. Gu^{1,59}, Y. T. Gu¹⁵, C. Y. Guan^{1,65}, A. Q. Guo³², L. B. Guo⁴², M. J. Guo⁵¹, R. P. Guo⁵⁰, Y. P. Guo^{12,g}, A. Guskov^{37,b}, J. Gutierrez²⁸, K. L. Han⁶⁵, T. T. Han¹, F. Hanisch³, K. D. Hao^{73,59}, X. Q. Hao²⁰, F. A. Harris⁶⁷, K. K. He⁵⁶, K. L. He^{1,65}, F. H. Heinsius³, C. H. Heinz³⁶, Y. K. Heng^{1,59,65}, C. Herold⁶¹, P. C. Hong³⁵, G. Y. Hou^{1,65}, X. T. Hou^{1,65}, Y. R. Hou⁶⁵, Z. L. Hou¹, H. M. Hu^{1,65}, J. F. Hu^{57,j}, Q. P. Hu^{73,59}, S. L. Hu^{12,g}, T. Hu^{1,59,65}, Y. Hu¹, Z. M. Hu⁶⁰, G. S. Huang^{73,59}, K. X. Huang⁶⁰, L. Q. Huang^{32,65}, P. Huang⁴³, X. T. Huang⁵¹, Y. P. Huang¹, Y. S. Huang⁶⁰, T. Hussain⁷⁵, N. Hüskens³⁶, N. in der Wiesche⁷⁰, J. Jackson²⁸, Q. Ji¹, Q. P. Ji²⁰, W. Ji^{1,65}, X. B. Ji^{1,65}, X. L. Ji^{1,59}, Y. Y. Ji⁵¹, Z. K. Jia^{73,59}, D. Jiang^{1,65}, H. B. Jiang⁷⁸, P. C. Jiang^{47,h}, S. J. Jiang⁹, T. J. Jiang¹⁷, X. S. Jiang^{1,59,65}, Y. Jiang⁶⁵, J. B. Jiao⁵¹, J. K. Jiao³⁵, Z. Jiao²⁴, S. Jin⁴³, Y. Jin⁶⁸, M. Q. Jing^{1,65}, X. M. Jing⁶⁵, T. Johansson⁷⁷, S. Kabana³⁴, N. Kalantar-Nayestanaki⁶⁶, X. L. Kang⁹, X. S. Kang⁴¹, M. Kavatsyuk⁶⁶, B. C. Ke⁸², V. Khachatryan²⁸, A. Khoukaz⁷⁰, R. Kiuchi¹, O. B. Kolcu^{63A}, B. Kopf³, M. Kuessner³, X. Kui^{1,65}, N. Kumar²⁷, A. Kupsc^{45,77}, W. Kühn³⁸, Q. Lan⁷⁴, W. N. Lan²⁰, T. T. Lei^{73,59}, M. Lellmann³⁶, T. Lenz³⁶, C. Li⁴⁴, C. Li⁴⁸, C. Li^{73,59}, C. H. Li⁴⁰, C. K. Li²¹, D. M. Li⁸², F. Li^{1,59}, G. Li¹, H. B. Li^{1,65}, H. J. Li²⁰, H. N. Li^{57,j}, Hui Li⁴⁴, J. R. Li⁶², J. S. Li⁶⁰, K. Li¹, K. L. Li²⁰, K. L. Li^{39,k,l}, L. J. Li^{1,65}, Lei Li⁴⁹, M. H. Li⁴⁴, M. R. Li^{1,65}, P. L. Li⁶⁵, P. R. Li^{39,k,l}, Q. M. Li^{1,65}, Q. X. Li⁵¹, R. Li^{18,32}, S. X. Li¹², T. Li⁵¹, T. Y. Li⁴⁴, W. D. Li^{1,65}, W. G. Li^{1,a}, X. Li^{1,65}, X. H. Li^{73,59}, X. L. Li⁵¹, X. Y. Li^{1,8}, X. Z. Li⁶⁰, Y. Li²⁰, Y. G. Li^{47,h}, Y. P. Li³⁵, Z. J. Li⁶⁰, Z. Y. Li⁸⁰, H. Liang^{73,59}, Y. F. Liang⁵⁵, Y. T. Liang^{32,65}, G. R. Liao¹⁴, L. B. Liao⁶⁰, M. H. Liao⁶⁰, Y. P. Liao^{1,65}, J. Libby²⁷, A. Limphirat⁶¹, C. C. Lin⁵⁶, D. X. Lin^{32,65}, L. Q. Lin⁴⁰, T. Lin¹, B. J. Liu¹, B. X. Liu⁷⁸, C. Liu³⁵, C. X. Liu¹, F. Liu¹, F. H. Liu⁵⁴, Feng Liu⁶, G. M. Liu^{57,j}, H. Liu^{39,k,l}, H. B. Liu¹⁵, H. H. Liu¹, H. M. Liu^{1,65}, Huihui Liu²², J. B. Liu^{73,59}, J. J. Liu²¹, K. Liu⁷⁴, K. Liu^{39,k,l}, K. Y. Liu⁴¹, Ke Liu²³, L. C. Liu⁴⁴, Lu Liu⁴⁴, M. H. Liu^{12,g}, P. L. Liu¹, Q. Liu⁶⁵, S. B. Liu^{73,59}, T. Liu^{12,g}, W. K. Liu⁴⁴, W. M. Liu^{73,59}, W. T. Liu⁴⁰, X. Liu⁴⁰, X. Liu^{39,k,l}, X. K. Liu^{39,k,l}, X. Y. Liu⁷⁸, Y. Liu⁸², Y. Liu⁸², Y. Liu^{39,k,l}, Y. B. Liu⁴⁴, Z. A. Liu^{1,59,65}, Z. D. Liu⁹, Z. Q. Liu⁵¹, X. C. Lou^{1,59,65}, F. X. Lu⁶⁰, H. J. Lu²⁴, J. G. Lu^{1,59}, X. L. Lu¹⁶, Y. Lu⁷, Y. H. Lu^{1,65}, Y. P. Lu^{1,59}, Z. H. Lu^{1,65}, C. L. Luo⁴², J. R. Luo⁶⁰, J. S. Luo^{1,65}, M. X. Luo⁸¹, T. Luo^{12,g}, X. L. Luo^{1,59}, Z. Y. Lv²³, X. R. Lyu^{65,p}, Y. F. Lyu⁴⁴, Y. H. Lyu⁸², F. C. Ma⁴¹, H. L. Ma¹, J. L. Ma^{1,65}, L. L. Ma⁵¹, L. R. Ma⁶⁸, Q. M. Ma¹, R. Q. Ma^{1,65}, R. Y. Ma²⁰, T. Ma^{73,59}, X. T. Ma^{1,65}, X. Y. Ma^{1,59}, Y. M. Ma³², F. E. Maas¹⁹, I. MacKay⁷¹, M. Maggiore^{76A,76C}, S. Malde⁷¹, Q. A. Malik⁷⁵, H. X. Mao^{39,k,l}, Y. J. Mao^{47,h}, Z. P. Mao¹, S. Marcello^{76A,76C}, A. Marshall⁶⁴, F. M. Melendi^{30A,30B}, Y. H. Meng⁶⁵, Z. X. Meng⁶⁸, G. Mezzadri^{30A}, H. Miao^{1,65}, T. J. Min⁴³, R. E. Mitchell²⁸, X. H. Mo^{1,59,65}, B. Moses²⁸, N. Yu. Muchnoi^{4,c}, J. Muskalla³⁶, Y. Nefedov³⁷, F. Nerling^{19,e}, L. S. Nie²¹, I. B. Nikolaev^{4,c}, Z. Ning^{1,59}, S. Nisar^{11,m}, Q. L. Niu^{39,k,l}, W. D. Niu^{12,g}, C. Normand⁶⁴, S. L. Olsen^{10,65}, Q. Ouyang^{1,59,65}, S. Pacetti^{29B,29C}, X. Pan⁵⁶, Y. Pan⁵⁸, A. Pathak¹⁰, Y. P. Pei^{73,59}, M. Pelizaeus³, H. P. Peng^{73,59}, X. J. Peng^{39,k,l}, Y. Y. Peng^{39,k,l}, K. Peters^{13,e}, K. Petridis⁶⁴, J. L. Ping⁴², R. G. Ping^{1,65}, S. Plura³⁶, V. Prasad³⁴, V. Prasad³⁵,

F. Z. Qi¹, H. R. Qi⁶², M. Qi⁴³, S. Qian^{1,59}, W. B. Qian⁶⁵, C. F. Qiao⁶⁵, J. H. Qiao²⁰, J. J. Qin⁷⁴, J. L. Qin⁵⁶, L. Q. Qin¹⁴, L. Y. Qin^{73,59}, P. B. Qin⁷⁴, X. P. Qin^{12,g}, X. S. Qin⁵¹, Z. H. Qin^{1,59}, J. F. Qiu¹, Z. H. Qu⁷⁴, J. Rademacker⁶⁴, C. F. Redmer³⁶, A. Rivetti^{76C}, M. Roloff^{76C}, G. Rong^{1,65}, S. S. Rong^{1,65}, F. Rosin^{29B,29C}, Ch. Rosner¹⁹, M. Q. Ruan^{1,59}, N. Salone⁴⁵, A. Sarantsev^{37,d}, Y. Schelhaas³⁶, K. Schoenning⁷⁷, M. Scodeggio^{30A}, K. Y. Shan^{12,g}, W. Shan²⁵, X. Y. Shan^{73,59}, Z. J. Shang^{39,k,l}, J. F. Shangguan¹⁷, L. G. Shao^{1,65}, M. Shao^{73,59}, C. P. Shen^{12,g}, H. F. Shen^{1,8}, W. H. Shen⁶⁵, X. Y. Shen^{1,65}, B. A. Shi⁶⁵, H. Shi^{73,59}, J. L. Shi^{12,g}, J. Y. Shi¹, S. Y. Shi⁷⁴, X. Shi^{1,59}, H. L. Song^{73,59}, J. J. Song²⁰, T. Z. Song⁶⁰, W. M. Song³⁵, Y. J. Song^{12,g}, Y. X. Song^{47,h,n}, S. Sosio^{76A,76C}, S. Spataro^{76A,76C}, F. Stieler³⁶, S. S. Su⁴¹, Y. J. Su⁶⁵, G. B. Sun⁷⁸, G. X. Sun¹, H. Sun⁶⁵, H. K. Sun¹, J. F. Sun²⁰, K. Sun⁶², L. Sun⁷⁸, S. S. Sun^{1,65}, T. Sun^{52,f}, Y. C. Sun⁷⁸, Y. H. Sun³¹, Y. J. Sun^{73,59}, Y. Z. Sun¹, Z. Q. Sun^{1,65}, Z. T. Sun⁵¹, C. J. Tang⁵⁵, G. Y. Tang¹, J. Tang⁶⁰, J. J. Tang^{73,59}, L. F. Tang⁴⁰, Y. A. Tang⁷⁸, L. Y. Tao⁷⁴, M. Tat⁷¹, J. X. Teng^{73,59}, J. Y. Tian^{73,59}, W. H. Tian⁶⁰, Y. Tian³², Z. F. Tian⁷⁸, I. Uman^{63B}, B. Wang¹, B. Wang⁶⁰, Bo Wang^{73,59}, C. Wang^{39,k,l}, C. Wang²⁰, Cong Wang²³, D. Y. Wang^{47,h}, H. J. Wang^{39,k,l}, J. J. Wang⁷⁸, K. Wang^{1,59}, L. L. Wang¹, L. W. Wang³⁵, M. Wang⁵¹, M. Wang^{73,59}, N. Y. Wang⁶⁵, S. Wang^{12,g}, T. Wang^{12,g}, T. J. Wang⁴⁴, W. Wang⁶⁰, W. Wang⁷⁴, W. P. Wang^{36,59,73,o}, X. Wang^{47,h}, X. F. Wang^{39,k,l}, X. J. Wang⁴⁰, X. L. Wang^{12,g}, X. N. Wang¹, Y. Wang⁶², Y. D. Wang⁴⁶, Y. F. Wang^{1,59,65}, Y. H. Wang^{39,k,l}, Y. J. Wang^{73,59}, Y. L. Wang²⁰, Y. N. Wang⁷⁸, Y. Q. Wang¹, Yaqian Wang¹⁸, Yi Wang⁶², Yuan Wang^{18,32}, Z. Wang^{1,59}, Z. L. Wang⁷⁴, Z. L. Wang², Z. Q. Wang^{12,g}, Z. Y. Wang^{1,65}, D. H. Wei¹⁴, H. R. Wei⁴⁴, F. Weidner⁷⁰, S. P. Wen¹, Y. R. Wen⁴⁰, U. Wiedner³, G. Wilkinson⁷¹, M. Wolke⁷⁷, C. Wu⁴⁰, J. F. Wu^{1,8}, L. H. Wu¹, L. J. Wu²⁰, L. J. Wu^{1,65}, Lianjie Wu²⁰, S. G. Wu^{1,65}, S. M. Wu⁶⁵, X. Wu^{12,g}, X. H. Wu³⁵, Y. J. Wu³², Z. Wu^{1,59}, L. Xia^{73,59}, X. M. Xian⁴⁰, B. H. Xiang^{1,65}, D. Xiao^{39,k,l}, G. Y. Xiao⁴³, H. Xiao⁷⁴, Y. L. Xiao^{12,g}, Z. J. Xiao⁴², C. Xie⁴³, K. J. Xie^{1,65}, X. H. Xie^{47,h}, Y. Xie⁵¹, Y. G. Xie^{1,59}, Y. H. Xie⁶, Z. P. Xie^{73,59}, T. Y. Xing^{1,65}, C. F. Xu^{1,65}, C. J. Xu⁶⁰, G. F. Xu¹, H. Y. Xu^{68,2}, H. Y. Xu², M. Xu^{73,59}, Q. J. Xu¹⁷, Q. N. Xu³¹, T. D. Xu⁷⁴, W. Xu¹, W. L. Xu⁶⁸, X. P. Xu⁵⁶, Y. Xu⁴¹, Y. Xu^{12,g}, Y. C. Xu⁷⁹, Z. S. Xu⁶⁵, F. Yan^{12,g}, H. Y. Yan⁴⁰, L. Yan^{12,g}, W. B. Yan^{73,59}, W. C. Yan⁸², W. H. Yan⁶, W. P. Yan²⁰, X. Q. Yan^{1,65}, H. J. Yang^{52,f}, H. L. Yang³⁵, H. X. Yang¹, J. H. Yang⁴³, R. J. Yang²⁰, T. Yang¹, Y. Yang^{12,g}, Y. F. Yang⁴⁴, Y. H. Yang⁴³, Y. Q. Yang⁹, Y. X. Yang^{1,65}, Y. Z. Yang²⁰, M. Ye^{1,59}, M. H. Ye⁸, Z. J. Ye^{57,j}, Junhao Yin⁴⁴, Z. Y. You⁶⁰, B. X. Yu^{1,59,65}, C. X. Yu⁴⁴, G. Yu¹³, J. S. Yu^{26,i}, L. Q. Yu^{12,g}, M. C. Yu⁴¹, T. Yu⁷⁴, X. D. Yu^{47,h}, Y. C. Yu⁸², C. Z. Yuan^{1,65}, H. Yuan^{1,65}, J. Yuan³⁵, J. Yuan⁴⁶, L. Yuan², S. C. Yuan^{1,65}, X. Q. Yuan¹, Y. Yuan^{1,65}, Z. Y. Yuan⁶⁰, C. X. Yue⁴⁰, Ying Yue²⁰, A. A. Zafar⁷⁵, S. H. Zeng^{64A,64B,64C,64D}, X. Zeng^{12,g}, Y. Zeng^{26,i}, Y. J. Zeng⁶⁰, Y. J. Zeng^{1,65}, X. Y. Zhai³⁵, Y. H. Zhan⁶⁰, A. Q. Zhang^{1,65}, B. L. Zhang^{1,65}, B. X. Zhang¹, D. H. Zhang⁴⁴, G. Y. Zhang^{1,65}, G. Y. Zhang²⁰, H. Zhang^{73,59}, H. Zhang⁸², H. C. Zhang^{1,59,65}, H. H. Zhang⁶⁰, H. Q. Zhang^{1,59,65}, H. R. Zhang^{73,59}, H. Y. Zhang^{1,59}, J. Zhang⁶⁰, J. Zhang⁸², J. J. Zhang⁵³, J. L. Zhang²¹, J. Q. Zhang⁴², J. S. Zhang^{12,g}, J. W. Zhang^{1,59,65}, J. X. Zhang^{39,k,l}, J. Y. Zhang¹, J. Z. Zhang^{1,65}, Jianyu Zhang⁶⁵, L. M. Zhang⁶², Lei Zhang⁴³, N. Zhang⁸², P. Zhang^{1,8}, Q. Zhang²⁰, Q. Y. Zhang³⁵, R. Y. Zhang^{39,k,l}, S. H. Zhang^{1,65}, Shulei Zhang^{26,i}, X. M. Zhang¹, X. Y. Zhang⁴¹, X. Y. Zhang⁵¹, Y. Zhang¹, Y. Zhang⁷⁴, Y. T. Zhang⁸², Y. H. Zhang^{1,59}, Y. M. Zhang⁴⁰, Y. P. Zhang^{73,59}, Z. D. Zhang¹, Z. H. Zhang¹, Z. L. Zhang³⁵, Z. L. Zhang⁵⁶, Z. X. Zhang²⁰, Z. Y. Zhang⁷⁸, Z. Y. Zhang⁴⁴, Z. Z. Zhang⁴⁶, Zh. Zh. Zhang²⁰, G. Zhao¹, J. Y. Zhao^{1,65}, J. Z. Zhao^{1,59}, L. Zhao^{73,59}, L. Zhao¹, M. G. Zhao⁴⁴, N. Zhao⁸⁰, R. P. Zhao⁶⁵, S. J. Zhao⁸², Y. B. Zhao^{1,59}, Y. L. Zhao⁵⁶, Y. X. Zhao^{32,65}, Z. G. Zhao^{73,59}, A. Zhemchugov^{37,b}, B. Zheng⁷⁴, B. M. Zheng³⁵, J. P. Zheng^{1,59}, W. J. Zheng^{1,65}, X. R. Zheng²⁰, Y. H. Zheng^{65,p}, B. Zhong⁴², C. Zhong²⁰, H. Zhou^{36,51,o}, J. Q. Zhou³⁵, J. Y. Zhou³⁵, S. Zhou⁶, X. Zhou⁷⁸, X. K. Zhou⁶, X. R. Zhou^{73,59}, X. Y. Zhou⁴⁰, Y. X. Zhou⁷⁹, Y. Z. Zhou^{12,g}, A. N. Zhu⁶⁵, J. Zhu⁴⁴, K. Zhu¹, K. J. Zhu^{1,59,65}, K. S. Zhu^{12,g}, L. Zhu³⁵, L. X. Zhu⁶⁵, S. H. Zhu⁷², T. J. Zhu^{12,g}, W. D. Zhu^{12,g}, W. D. Zhu⁴², W. J. Zhu¹, W. Z. Zhu²⁰, Y. C. Zhu^{73,59}, Z. A. Zhu^{1,65}, X. Y. Zhuang⁴⁴, J. H. Zou¹, J. Zu^{73,59}

(BESIII Collaboration)

¹ Institute of High Energy Physics, Beijing 100049, People's Republic of China

² Beihang University, Beijing 100191, People's Republic of China

³ Bochum Ruhr-University, D-44780 Bochum, Germany

⁴ Budker Institute of Nuclear Physics SB RAS (BINP), Novosibirsk 630090, Russia

⁵ Carnegie Mellon University, Pittsburgh, Pennsylvania 15213, USA

⁶ Central China Normal University, Wuhan 430079, People's Republic of China

⁷ Central South University, Changsha 410083, People's Republic of China

- ⁸ China Center of Advanced Science and Technology, Beijing 100190, People's Republic of China
⁹ China University of Geosciences, Wuhan 430074, People's Republic of China
¹⁰ Chung-Ang University, Seoul, 06974, Republic of Korea
¹¹ COMSATS University Islamabad, Lahore Campus, Defence Road, Off Raiwind Road, 54000 Lahore, Pakistan
¹² Fudan University, Shanghai 200433, People's Republic of China
¹³ GSI Helmholtzcentre for Heavy Ion Research GmbH, D-64291 Darmstadt, Germany
¹⁴ Guangxi Normal University, Guilin 541004, People's Republic of China
¹⁵ Guangxi University, Nanning 530004, People's Republic of China
¹⁶ Guangxi University of Science and Technology, Liuzhou 545006, People's Republic of China
¹⁷ Hangzhou Normal University, Hangzhou 310036, People's Republic of China
¹⁸ Hebei University, Baoding 071002, People's Republic of China
¹⁹ Helmholtz Institute Mainz, Staudinger Weg 18, D-55099 Mainz, Germany
²⁰ Henan Normal University, Xinxiang 453007, People's Republic of China
²¹ Henan University, Kaifeng 475004, People's Republic of China
²² Henan University of Science and Technology, Luoyang 471003, People's Republic of China
²³ Henan University of Technology, Zhengzhou 450001, People's Republic of China
²⁴ Huangshan College, Huangshan 245000, People's Republic of China
²⁵ Hunan Normal University, Changsha 410081, People's Republic of China
²⁶ Hunan University, Changsha 410082, People's Republic of China
²⁷ Indian Institute of Technology Madras, Chennai 600036, India
²⁸ Indiana University, Bloomington, Indiana 47405, USA
²⁹ INFN Laboratori Nazionali di Frascati , (A)INFN Laboratori Nazionali di Frascati, I-00044, Frascati, Italy; (B)INFN Sezione di Perugia, I-06100, Perugia, Italy; (C)University of Perugia, I-06100, Perugia, Italy
³⁰ INFN Sezione di Ferrara, (A)INFN Sezione di Ferrara, I-44122, Ferrara, Italy; (B)University of Ferrara, I-44122, Ferrara, Italy
³¹ Inner Mongolia University, Hohhot 010021, People's Republic of China
³² Institute of Modern Physics, Lanzhou 730000, People's Republic of China
³³ Institute of Physics and Technology, Mongolian Academy of Sciences, Peace Avenue 54B, Ulaanbaatar 13330, Mongolia
³⁴ Instituto de Alta Investigación, Universidad de Tarapacá, Casilla 7D, Arica 1000000, Chile
³⁵ Jilin University, Changchun 130012, People's Republic of China
³⁶ Johannes Gutenberg University of Mainz, Johann-Joachim-Becher-Weg 45, D-55099 Mainz, Germany
³⁷ Joint Institute for Nuclear Research, 141980 Dubna, Moscow region, Russia
³⁸ Justus-Liebig-Universitaet Giessen, II. Physikalisches Institut, Heinrich-Buff-Ring 16, D-35392 Giessen, Germany
³⁹ Lanzhou University, Lanzhou 730000, People's Republic of China
⁴⁰ Liaoning Normal University, Dalian 116029, People's Republic of China
⁴¹ Liaoning University, Shenyang 110036, People's Republic of China
⁴² Nanjing Normal University, Nanjing 210023, People's Republic of China
⁴³ Nanjing University, Nanjing 210093, People's Republic of China
⁴⁴ Nankai University, Tianjin 300071, People's Republic of China
⁴⁵ National Centre for Nuclear Research, Warsaw 02-093, Poland
⁴⁶ North China Electric Power University, Beijing 102206, People's Republic of China
⁴⁷ Peking University, Beijing 100871, People's Republic of China
⁴⁸ Qufu Normal University, Qufu 273165, People's Republic of China
⁴⁹ Renmin University of China, Beijing 100872, People's Republic of China
⁵⁰ Shandong Normal University, Jinan 250014, People's Republic of China
⁵¹ Shandong University, Jinan 250100, People's Republic of China
⁵² Shanghai Jiao Tong University, Shanghai 200240, People's Republic of China
⁵³ Shanxi Normal University, Linfen 041004, People's Republic of China
⁵⁴ Shanxi University, Taiyuan 030006, People's Republic of China
⁵⁵ Sichuan University, Chengdu 610064, People's Republic of China

⁵⁶ *Soochow University, Suzhou 215006, People's Republic of China*

⁵⁷ *South China Normal University, Guangzhou 510006, People's Republic of China*

⁵⁸ *Southeast University, Nanjing 211100, People's Republic of China*

⁵⁹ *State Key Laboratory of Particle Detection and Electronics,
Beijing 100049, Hefei 230026, People's Republic of China*

⁶⁰ *Sun Yat-Sen University, Guangzhou 510275, People's Republic of China*

⁶¹ *Suranaree University of Technology, University Avenue 111, Nakhon Ratchasima 30000, Thailand*

⁶² *Tsinghua University, Beijing 100084, People's Republic of China*

⁶³ *Turkish Accelerator Center Particle Factory Group, (A)Istinye University, 34010, Istanbul,
Turkey; (B)Near East University, Nicosia, North Cyprus, 99138, Mersin 10, Turkey*

⁶⁴ *University of Bristol, H H Wills Physics Laboratory, Tyndall Avenue, Bristol, BS8 1TL, UK*

⁶⁵ *University of Chinese Academy of Sciences, Beijing 100049, People's Republic of China*

⁶⁶ *University of Groningen, NL-9747 AA Groningen, The Netherlands*

⁶⁷ *University of Hawaii, Honolulu, Hawaii 96822, USA*

⁶⁸ *University of Jinan, Jinan 250022, People's Republic of China*

⁶⁹ *University of Manchester, Oxford Road, Manchester, M13 9PL, United Kingdom*

⁷⁰ *University of Muenster, Wilhelm-Klemm-Strasse 9, 48149 Muenster, Germany*

⁷¹ *University of Oxford, Keble Road, Oxford OX13RH, United Kingdom*

⁷² *University of Science and Technology Liaoning, Anshan 114051, People's Republic of China*

⁷³ *University of Science and Technology of China, Hefei 230026, People's Republic of China*

⁷⁴ *University of South China, Hengyang 421001, People's Republic of China*

⁷⁵ *University of the Punjab, Lahore-54590, Pakistan*

⁷⁶ *University of Turin and INFN, (A)University of Turin, I-10125, Turin, Italy; (B)University
of Eastern Piedmont, I-15121, Alessandria, Italy; (C)INFN, I-10125, Turin, Italy*

⁷⁷ *Uppsala University, Box 516, SE-75120 Uppsala, Sweden*

⁷⁸ *Wuhan University, Wuhan 430072, People's Republic of China*

⁷⁹ *Yantai University, Yantai 264005, People's Republic of China*

⁸⁰ *Yunnan University, Kunming 650500, People's Republic of China*

⁸¹ *Zhejiang University, Hangzhou 310027, People's Republic of China*

⁸² *Zhengzhou University, Zhengzhou 450001, People's Republic of China*

^a Deceased

^b Also at the Moscow Institute of Physics and Technology, Moscow 141700, Russia

^c Also at the Novosibirsk State University, Novosibirsk, 630090, Russia

^d Also at the NRC "Kurchatov Institute", PNPI, 188300, Gatchina, Russia

^e Also at Goethe University Frankfurt, 60323 Frankfurt am Main, Germany

^f Also at Key Laboratory for Particle Physics, Astrophysics and Cosmology, Ministry
of Education; Shanghai Key Laboratory for Particle Physics and Cosmology; Institute
of Nuclear and Particle Physics, Shanghai 200240, People's Republic of China

^g Also at Key Laboratory of Nuclear Physics and Ion-beam Application (MOE) and
Institute of Modern Physics, Fudan University, Shanghai 200443, People's Republic of China

^h Also at State Key Laboratory of Nuclear Physics and Technology,
Peking University, Beijing 100871, People's Republic of China

ⁱ Also at School of Physics and Electronics, Hunan University, Changsha 410082, China

^j Also at Guangdong Provincial Key Laboratory of Nuclear Science, Institute
of Quantum Matter, South China Normal University, Guangzhou 510006, China

^k Also at MOE Frontiers Science Center for Rare Isotopes,
Lanzhou University, Lanzhou 730000, People's Republic of China

^l Also at Lanzhou Center for Theoretical Physics, Lanzhou University, Lanzhou 730000, People's Republic of China

^m Also at the Department of Mathematical Sciences, IBA, Karachi 75270, Pakistan

ⁿ Also at Ecole Polytechnique Federale de Lausanne (EPFL), CH-1015 Lausanne, Switzerland

^o Also at Helmholtz Institute Mainz, Staudinger Weg 18, D-55099 Mainz, Germany

^p Also at Hangzhou Institute for Advanced Study, University of Chinese Academy of Sciences, Hangzhou 310024, China

FIT RESULTS WITH ALTERNATIVE MODELS.

TABLE I. Fit results with alternative models. “BW” represents resonance structures with mass and width kept float, “PS” represents the phase space term. The column referred to as “w/o model” represents the model with one contribution removed, while “The extra” is the removed contribution.

Model	w/o model	The extra / Significance
2BW + PS/ s^n	2BW	PS/ s^n / 1.3σ
3BW	2BW	BW / 5.4σ
3BW + PS/ s^n	2BW + PS/ s^n	BW / 5.1σ
	3BW	PS/ s^n / 0.1σ
4BW	3BW	BW / 0.7σ

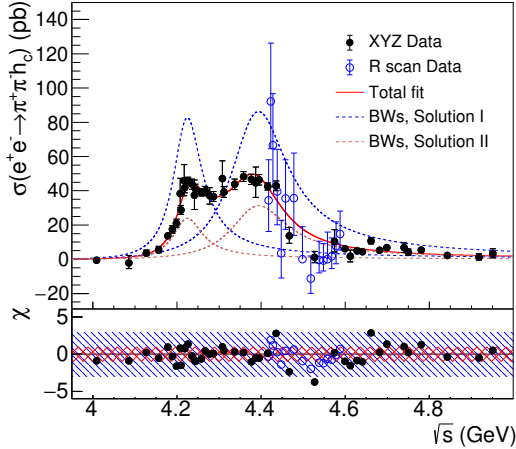


FIG. 1. The \sqrt{s} -dependent cross section lineshape described by the coherent sum of two BW functions (the red curve). The blue and red dashed curves are contributions from the two structures. The dots with error bars are data. The bottom panel shows the χ values.

NUMERICAL RESULTS AT EACH DATA SAMPLE

TABLE II. Comparison of parameters of the resonances from the previous measurement [1] (or PDG) and this measurement described by using a coherent sum of two or three BW functions. The first error comes from statistics and the second is the systematic uncertainty. Under the same fit method, this measurement improve the statistical uncertainty. The widths of the two structures are both wider, while still within agreement as the previous measurement. After taken R_3 into consideration, the resonance parameters of R_1 and R_2 change.

Resonance	Parameter	this work (3BW)	this work (2BW)	previous work
R_1	M (MeV/ c^2)	$4223.6^{+3.6+2.6}_{-3.7-2.9}$	$4220.6^{+3.4}_{-3.5}$	$4218.4 \pm 4.0 \pm 0.9$
	Γ_{tot} (MeV)	$58.5^{+10.8+6.7}_{-11.4-6.5}$	$84.5^{+5.8}_{-5.3}$	$66.0 \pm 9.0 \pm 0.4$
R_2	M (MeV/ c^2)	$4327.4^{+20.4+10.7}_{-18.8-9.3}$	$4383.5^{+6.1}_{-6.0}$	$4391.6 \pm 6.3 \pm 1.0$
	Γ_{tot} (MeV)	$244.1^{+34.0+24.3}_{-27.1-18.3}$	$162.5^{+10.9}_{-10.2}$	$139.5 \pm 16.1 \pm 0.6$
R_3	M (MeV/ c^2)	$4467.4^{+7.2+3.2}_{-5.4-2.7}$	—	4421 ± 4
	Γ_{tot} (MeV)	$62.8^{+19.2+9.9}_{-14.4-7.0}$	—	62 ± 20 (from PDG)
	χ^2/ndf	41.9/70	77.9/66	—

TABLE III. Numerical results for each energy point. The data samples are divided into two classes according to the integrated luminosity and the cross section line shape: the 19 data points with a large number of signal events (the upper half), and the other 25 points ((the lower half). Shown are also the integral luminosity \mathcal{L} , the number of signal events N_{sig} , the weighted efficiency $\sum_{i=1}^{16} \epsilon_i \cdot \mathcal{B}_i$, the radiative correction factor $1 + \delta$, and the dressed cross section σ^{dressed} . For “ σ^{dressed} ”, the first error is statistical, the second error is the systematic, and the third error comes from the input branching ratios which is the dominant one in the multiplicative systematic uncertainties.

\sqrt{s} (GeV)	\mathcal{L} (pb $^{-1}$)	N_{sig}	$\sum_{i=1}^{16} \epsilon_i \cdot \mathcal{B}_i$ (%)	$1 + \delta$	σ^{dressed}
4.189	570	158 ± 19	3.86	0.750	$17.7 \pm 2.1 \pm 1.6 \pm 1.7$
4.199	526	178 ± 20	3.93	0.744	$21.3 \pm 2.3 \pm 2.8 \pm 2.1$
4.209	517	234 ± 21	3.88	0.740	$29.1 \pm 2.7 \pm 1.6 \pm 2.8$
4.219	515	342 ± 24	3.89	0.743	$42.4 \pm 3.0 \pm 2.4 \pm 4.1$
4.236	530	394 ± 26	4.00	0.779	$43.9 \pm 2.9 \pm 2.4 \pm 4.3$
4.244	538	377 ± 26	3.96	0.801	$40.7 \pm 2.8 \pm 2.3 \pm 3.9$
4.267	531	369 ± 26	3.85	0.836	$39.8 \pm 2.8 \pm 2.2 \pm 3.9$
4.278	176	111 ± 14	3.75	0.839	$37.0 \pm 4.8 \pm 2.1 \pm 3.6$
4.178	3189	699 ± 41	3.85	0.757	$13.8 \pm 0.8 \pm 0.8 \pm 1.3$
4.287	502	302 ± 24	3.59	0.839	$36.7 \pm 2.9 \pm 2.0 \pm 3.6$
4.311	501	329 ± 26	3.64	0.837	$39.7 \pm 3.1 \pm 2.2 \pm 3.8$
4.337	505	378 ± 27	3.75	0.841	$43.7 \pm 3.1 \pm 2.4 \pm 4.2$
4.377	523	423 ± 27	3.72	0.859	$46.7 \pm 3.0 \pm 2.9 \pm 4.5$
4.395	508	411 ± 27	3.68	0.870	$46.6 \pm 3.1 \pm 2.9 \pm 4.5$
4.436	570	436 ± 29	3.64	0.904	$42.9 \pm 2.9 \pm 2.7 \pm 4.2$
4.226	1101	847 ± 38	4.05	0.755	$46.3 \pm 2.1 \pm 2.6 \pm 4.5$
4.258	828	569 ± 32	3.93	0.828	$38.9 \pm 2.2 \pm 2.2 \pm 3.8$
4.358	544	472 ± 28	3.90	0.850	$48.2 \pm 2.9 \pm 3.0 \pm 4.7$
4.416	1091	831 ± 41	3.74	0.882	$42.6 \pm 2.1 \pm 2.7 \pm 4.1$
4.127	402	21^{+11}_{-10}	3.60	0.773	$3.5^{+1.9}_{-1.7} \pm 0.8 \pm 0.3$
4.157	409	36^{+13}_{-12}	3.72	0.766	$5.7^{+2.0}_{-1.9} \pm 0.7 \pm 0.6$
4.009	482	-5^{+8}_{-7}	3.54	0.774	$-0.7^{+1.1}_{-1.0} \pm 0.1 \pm 0.1$
4.467	111	30^{+11}_{-10}	3.05	1.255	$13.2^{+4.6+1.7}_{-4.3-1.5} \pm 1.3$
4.527	112	3^{+7}_{-6}	1.45	2.194	$1.4^{+3.5+0.9}_{-3.2-0.9} \pm 0.1$
4.574	49	9^{+6}_{-5}	2.42	1.381	$10.5^{+7.0}_{-6.1} \pm 1.4 \pm 1.0$
4.600	587	67^{+18}_{-17}	2.60	1.304	$6.2^{+1.7}_{-1.6} \pm 0.5 \pm 0.6$
4.308	45	37^{+8}_{-8}	3.88	0.837	$47.2^{+10.4}_{-9.5} \pm 3.6 \pm 4.6$
4.208	55	35^{+8}_{-7}	4.07	0.740	$39.0^{+9.0}_{-8.2} \pm 2.7 \pm 3.8$
4.217	55	42^{+9}_{-8}	4.08	0.742	$46.6^{+8.6}_{-8.0} \pm 2.6 \pm 4.5$
4.242	56	36^{+9}_{-8}	4.02	0.795	$37.3^{+9.0}_{-8.3} \pm 2.1 \pm 3.6$
4.085	53	-2^{+4}_{-3}	3.70	0.776	$-2.2^{+4.5}_{-3.4} \pm 0.2 \pm 0.2$
4.387	56	45^{+9}_{-9}	3.87	0.865	$44.8^{+9.3}_{-8.5} \pm 3.3 \pm 4.3$
4.612	104	3^{+7}_{-6}	2.55	1.287	$1.7^{+3.7}_{-3.2} \pm 0.4 \pm 0.2$
4.628	522	46^{+16}_{-15}	2.58	1.269	$4.9^{+1.7}_{-1.7} \pm 0.3 \pm 0.5$
4.641	552	43^{+17}_{-16}	2.61	1.263	$4.3^{+1.7}_{-1.6} \pm 0.4 \pm 0.4$
4.661	529	103^{+18}_{-17}	2.65	1.257	$10.7^{+1.9}_{-1.8} \pm 0.6 \pm 1.0$
4.682	1667	155^{+29}_{-28}	2.65	1.255	$5.1^{+1.0}_{-0.9} \pm 0.3 \pm 0.5$
4.699	536	65^{+17}_{-16}	2.66	1.255	$6.7^{+1.7}_{-1.6} \pm 0.4 \pm 0.7$
4.740	165	21^{+9}_{-8}	2.74	1.257	$6.7^{+2.9}_{-2.7} \pm 0.4 \pm 0.7$
4.750	367	28^{+13}_{-13}	2.76	1.260	$4.1^{+1.9}_{-1.8} \pm 0.3 \pm 0.4$
4.781	511	52^{+16}_{-16}	2.75	1.263	$5.4^{+1.7}_{-1.6} \pm 0.4 \pm 0.5$
4.843	525	22^{+14}_{-14}	2.76	1.271	$2.2^{+1.4}_{-1.4} \pm 0.2 \pm 0.2$
4.918	208	5^{+8}_{-7}	2.74	1.286	$1.3^{+2.0}_{-1.8} \pm 0.1 \pm 0.1$
4.951	159	10^{+8}_{-8}	2.68	1.293	$3.4^{+2.7}_{-2.5} \pm 0.6 \pm 0.3$

TABLE IV. Numerical results at each R-scan energy. The “ $\sigma_{\text{U.L.}}^{\text{dressed}}$ ” represent the upper limit of σ^{dressed} , the numbers in brackets are the most conservative result after taking systematic uncertainties into account. At 4558 the fit quality is not good, so only an U.L. at the 90% C.L. is given.

\sqrt{s} (GeV)	\mathcal{L} (pb $^{-1}$)	N_{sig}	$\sum_{i=1}^{16} \epsilon_i \cdot \mathcal{B}_i$ (%)	$1+\delta$	σ^{dressed}	$\sigma_{\text{U.L.}}^{\text{dressed}}$
4.418	7.5	5_{-2}^{+3}	3.73	0.884	$34.6_{-18.5}^{+23.9} \pm 2.2 \pm 3.4$	< 72.9(< 73.8)
4.423	7.4	12_{-4}^{+5}	3.72	0.889	$93.5_{-28.1}^{+34.5} \pm 5.8 \pm 9.1$	< 144.6(< 147.7)
4.428	6.8	8_{-3}^{+4}	3.70	0.894	$67.5_{-24.9}^{+30.7} \pm 4.2 \pm 6.5$	< 114.9(< 116.8)
4.438	7.6	5_{-3}^{+3}	3.63	0.909	$40.2_{-19.9}^{+25.2} \pm 2.5 \pm 3.9$	< 79.8(< 80.8)
4.448	7.7	1_{-2}^{+3}	3.54	0.945	$3.7_{-14.7}^{+19.9} \pm 0.2 \pm 0.4$	< 42.0(< 42.2)
4.458	8.7	6_{-3}^{+4}	3.35	1.035	$36.4_{-18.5}^{+23.1} \pm 2.7 \pm 3.5$	< 72.3(< 73.3)
4.478	8.2	7_{-4}^{+5}	2.11	2.287	$30.6_{-19.5}^{+23.5} \pm 14.5 \pm 3.0$	< 66.2(< 77.9)
4.498	8.0	0_{-3}^{+4}	0.40	133.2	$0.1_{-1.5}^{+1.7} \pm 5.5 \pm 0$	< 3.3(< 105.1)
4.518	8.7	-2_{-1}^{+2}	1.05	3.066	$-12.0_{-9.5}^{+15.0} \pm 0.8 \pm 1.1$	< 29.1(< 29.3)
4.538	9.3	0_{-2}^{+2}	1.82	1.777	$0.2_{-0.3}^{+13.7} \pm 0 \pm 0$	< 28.8(< 28.9)
4.548	8.8	0_{-1}^{+2}	2.06	1.588	$-0.8_{-7.2}^{+11.8} \pm 0 \pm 0.1$	< 25.9(< 26.0)
4.558	8.3	< 3	2.24	1.478	—	< 18.9(< 18.9)
4.568	8.4	0_{-1}^{+2}	2.36	1.410	$2.2_{-8.8}^{+13.0} \pm 0.1 \pm 0.2$	< 29.1(< 29.2)
4.578	8.5	2_{-2}^{+3}	2.45	1.368	$9.7_{-12.6}^{+17.4} \pm 0.6 \pm 0.9$	< 40.9(< 41.1)
4.588	8.2	3_{-2}^{+2}	2.52	1.336	$17.7_{-11.3}^{+16.1} \pm 1.1 \pm 1.7$	< 45.8(< 46.2)

-
- [1] M. Ablikim *et al.* (BESIII Collaboration), Phys. Rev. Lett. **118** (2017) 092002.